TEMPERATURE MEASUREMENT OF AN ATMOSPHERIC ARGON PLASMA JET USING AN INTERMITTENT THERMOCOUPLE TECHNIQUE

BY

CHUNG-CHING CHIANG

A Thesis

Submitted to the Faculty of

Science and Engineering

of the University of Ottawa

in Partial Fulfillment of the

Requirements for the

Degree of

MASTER OF APPLIED SCIENCE

In Mechanical Engineering

September, 1970

ABSTRACT

A low power, atmospheric, argon, plasma jet was built. An intermittent thermocouple driven by a double acting solenoid and cooled by a water-jacket was used to measure the atmospheric argon plasma temperature. It was necessary to use a large bead of 0.063 inch diameter to reduce the probe response. The radiation heat lost by this probe to the surroundings was estimated to be negligibly small. By keeping the ratio of the diameter to the length of the lead less than 0.1, the conduction heat lost from the bead to the base of the leads could be neglected. A factorial plan method was applied to analyse the temperature characteristics of a 0.125 inch nozzle plasma jet and an empirical equation was developed to describe changes with gas flow rate, arc current and distance along the axis of the jet. Deviation between this equation and experimental results is within 10 %.

ACKNOWLEDGEMENT

The author wishes to express gratitude to Dr. R. P. Henry of the Department of Mechanical Engineering of the University of Ottawa for his very thoughtful advice and useful help in carrying out this research, also the author wishes to extend his grateful thanks to Mr. Stephen So who did the typing.

The studies reported herein were supported by funds from the National Research Council of Canada Grant Number 8556.

TABLE OF CONTENTS

LIST OF SYMBOLS

A_b	Mean surface area of the bead
A_w	Cross-sectional area of the wire leads
B	Probe
C_b	Specific heat of the bead
C_{pa}	Specific heat of argon plasma at constant pressure
D	Diameter of the arc jet nozzle
D_b	Diameter of the bead
D_w	Diameter of the wire leads
F	Flow rate
F_1	Flow rate of argon plasma at temperature T_1
F_4	Flow rate of argon gas coming out from the flow meter
F_5	Flow rate of argon plasma at the arc jet nozzle
Gr_f	Grashof number of air
H	Ratio of α_o to α_m
K_a	Thermal conductivity of argon plasma
K_{al}	Thermal conductivity of alumel
K_{ch}	Thermal conductivity of chromel
K_f	Thermal conductivity of air
K_w	Thermal conductivity of the average value of K_{ch} and K_{al}
L_w	Length of the wire leads
M_5	Mach number of argon plasma at the arc jet nozzle
Nu_a	Nusselt number of argon plasma
Nu_f	Nusselt number of air
P	Pressure

P_1	Argon plasma pressure at point 1
P_4	Argon gas pressure at point 4
P_5	Argon plasma pressure at point 5
Pr_a	Prandtl number of argon plasma
Pr_f	Prandtl number of air
Q	Heat transfer rate
Q_c	Convective heat transfer rate
Q_k	Conductive heat transfer rate
Q_r	Radiative heat transfer rate
R	Cycling ratio = b/a
R_1	Reservoir at high temperature
R_3	Reservoir at low temperature
Re	Reynolds number
T_1	Temperature of the hot gas
T_2	Instantaneous temperature of the probe
$\overline{T}_2$	Average probe temperature = $\frac{1}{2}$ $(T_m + T_o)$
T_3	Temperature of R_3
T_4	Temperature of argon gas at P_4
T_5	Temperature of argon plasma at P_5
T_m	Maximum probe temperature
T_o	Minimum probe temperature
T_R	Reservoir temperature (T_1 or T_3)
T_r	Room temperature
T_w	Wire lead temperature
T_{wb}	Lead base temperature
U_1	Velocity of argon plasma at T_i
U_5	Velocity of argon plasma at T_5

$\forall_b$	Volume of the bead
X	Distance
W	Arbitrary constant
a	Period of time when the probe is set in the hot gas
a_5	Sonic velocity of argon plasma at T_5
b	Period of time when the probe is set in the water-cooled jacket
c	Arbitrary constant
g	Acceleration of gravity
h	Surface heat transfer coefficient of the probe
h_m	Surface heat transfer coefficient of the probe at T_m
h_o	Surface heat transfer coefficient of the probe at T_o
m	Arbitrary constant
q	Heat
t	Time
z	Variable in series
α_b	Absorptivity of the bead
α_m	$(h_m A_b)/(\rho_b C_{pb} V_b)$
α_o	$(h_o A_b)/(\rho_b C_{pb} V_b)$
β_f	Volume coefficient of expansion of air
ϵ_b	Emissivity of the bead
θ_1	$(T_1 - T_3)$
$\bar{\theta}_2$	$(\bar{T}_2 - T_3)$
μ_a	Viscosity of the argon plasma
ν_f	Kinematic viscosity of air
ρ_3	Density of air at T_3
ρ_a	Density of argon plasma
ρ_f	Density of air at $\frac{1}{2}(T_o + T_3)$

σ Stefan-Boltzmann constant

τ Period = a + b

LIST OF FIGURES

1. INTRODUCTION

1.1 Preamble

The conventional way of measuring moderate gas temperatures is by placing a thermocouple in thermal equilibrium with the gas. At the extremely high temperature of plasmas, any kind of thermal material would melt away. Microwave and spectroscopic techniques measure the plasma temperature without setting any solid material inside the hot flame. However using these techniques, only an average temperature across a section of the plasma can be measured. For local temperature measurement, one of the most promising new techniques is the use of an intermittent thermocouple.

The bead of this thermocouple is pulsed into the point of interest in the plasma flame, but is then pulled back into the cool reservoir before it reaches its melting point. By using two different pulse rates, one can eliminate unknow probe properties and easily evaluate the local plasma temperatures.

1.2 Previous Work

There are several ways of measuring arc jet plasma temperature. Two of the most widely used and accurate methods employ spectroscopic and microwave diagnostic techniques.

Another way involves the rapid rotation of an electrostatic probe through the plasma flame. In this method, the period of rotation is rapid enough so that the probe does not melt (1) (Figure 1). These techniques measure only the average temperature across a section of plasma. For local temperature measurement, the only way is to set a probe into the plasma at the particular point of interest; however all conventional thermocouples would melt away at the extremely high plasma temperatures. This necessitates the cooling of the probe so that the probe does not reach its melting point. A water-cooled calorimeter probe was first developed by Grey (2) for plasma temperature measurement. Later on, a cooled electrostatic probe was introduced by Grey and Jacobs (3) This probe not only measured the local plasma temperature but also the electron density and ion density. These two kinds of probes now are commercially available on the market.

Since they are very complicated precision instruments, these probes are very expensive and require an elaborate monitoring and indicating system. Another simpler and cheaper instrument promises to do the same job of measuring local hot gas temperature as this expensive probe. This is the intermittent thermocouple. This probe was first employed by Raezer and Olsen (4) for atmospheric argon plasma jet temperature measurement and then by Henry (5) for low-pressure argon plasma-accelerator diagnosis.

1.3 Principle of the Intermittent Thermocouple

In temperature region above the melting point of metals, no conventional thermocouple can be used for measurement of extremely hot gas temperature by setting it in thermal equilibrium with the hot gas.

Consider a material body composed of a chemically inert and non-catalytic material (e.g. chromel-alumel thermocouple). Let this body be placed in a stream of extremely hot gas and allow it to remain in the hot gas for a period of time long on the scale of molecular events but not long enough for the surface to melt. The heat transfer between the gas and the body will depend in some manner on the sum of the average kinetic and thermal energy of the gas and also depend upon the body cycling rate into and out of the hot gas.

Knowing the mechanisms of heat transfer, one can derive the hot gas temperature from the much lower thermocouple mean temperature. Raezer and Olsen neglected radiation and conduction heat losses, considering convection to be the dominating means of heat transfer. Radiation heat loss would be that radiated from the surface of the probe to the surroundings. Also, radiation heat gained from the hot gas by the probe was neglected. The conduction heat loss would be that conducted from the probe through the leads. In their analysis, Raezer and Olsen used the following assumptions:

(a) The plasma was assumed to be optically thin so that the absorptivity of the plasma was negligibly small. Consequently no radiation energy from the probe surface to the surroundings was absorbed by the plasma and no radiation energy was absorbed by the probe from the plasma. Besides, the temperature difference between the probe surface and the surroundings was not too high, therefore, the radiation heat loss was neglected.

(b) The ratio between the diameter of the leads and the length of the leads of the probe was very small, so that, the conduction heat lost from the probe tip down to the base of the leads could be neglected.

However, Henry, working in a vacuum system, found that in his studies the conduction heat loss was significant. The radiation heat loss in his system was assumed to be negligibly small.

The cycling techniques employed in References (4) and (5) were different. Raezer and Olsen used a light source, chopper wheel, photocell and amplifier to generate an output to operate the relays which controlled the driving current through a double-acting solenoid (Figure 2). This method had been first employed in Reference (6) to measure the average temperature of flame kernels. Henry made an electronic power switching circuit and timing circuit to control the driving current through a double acting solenoid (Figure3). Since this latter timing circuit was more convenient for use

in this experiment, Henry's method was applied with a modification to increase the cycling ratio R = b/a.

1.4 Objective of Experiment

A low power, atmospheric, argon, plasma jet was constructed. Plasma temperatures were measured along the axis of the arc jet at different gas flow rates with different arc currents and with two different sizes of nozzles. The results were analysed by the method of factorial plan (7) to establish an algebraic equation for the temperature of the hot gas as a function of arc current, gas flow rate and distance along the axis of arc jet. The temperature of the plasma was predicted as follows.

Using three different values of R, three different traces of the probe response were obtained. The combination of any two results of these traces yields three different approximate values of the hot gas temperature. If these values differed by less than 5%, then the average value of these three was accepted as the value of the plasma temperature at that specific condition of arc current, gas flow rate and distance along the axis of the arc jet.

The temperature profiles of argon plasma along the axis of the arc jet were taken for two different nozzle diameters. The relation between the size of the nozzle and the temperature was examined. The diameter of the beads of the probe was

changed to see the effect on temperature measurement. Heat losses by both radiation and conduction were estimated and found to be negligibly small in the atmospheric pressure arc jet (Refer to Section 2-3).

2. THEORY

Using basic ideas of heat transfer, energy balance and elementary differential equations, one can relate the very hot gas temperature to the much lower steady state thermocouple temperature indication.

2.1 Derivation of the Probe Heat Transfer Relation

Consider two reservoirs R_1 and R_3 maintained at temperature T_1 and T_3 respectively. Let a thermocouple B pass in a periodic manner with period τ between the two reservoirs, spending a time "a" in R_1 and a time "b" in R_3, with negligible time spent travelling from one reservoir to the other. Let T_2 be the instantaneous temperature of B. After sufficient cycling between the two reservoirs, the mean probe temperature will approach a constant value $\bar{T}_2$. Under these conditions, the heat gained by B during the time it spends in R_1 is equal to the heat it loses during the time it is in R_3. Figure 4 illustrates the probe cyclical motion and corresponding thermocouple output.

Hence,
$$\int_0^a Q_{1,2}\, dt = \int_a^\tau Q_{2,3}\, dt \qquad (1)$$

where heat fluxes:
$$Q_{1,2} = f_{fn}(T_1 - T_2)$$
$$Q_{2,3} = f_{fr}(T_2 - T_3)$$

At any instant dt during probe cycling, conservation of energy yields:

$$Q_c + Q_k + Q_r = Q_s \tag{2}$$

where the rates Q are:

convective heat gained or lost by the probe

$$Q_c = h A_b (T_R - T_2) \tag{3}$$

conductive heat lost by the probe to the base of the leads

$$Q_k = -2 K_w A_w \frac{dT_w}{dx} \tag{4}$$

radiative heat lost by the probe (based on assumptions (a) and (b) given below).

$$Q_r = \sigma A_b (\epsilon_b T_2^4 - \alpha_b T_r^4) \tag{5}$$

heat storage in the probe

$$Q_s = V_b \rho_b C_b \frac{dT_2}{dt} \tag{6}$$

The assumptions for radiative heat loss are as follows:

(a) The surroundings are black body.

(b) The absorptivity and emissivity of the hot gas are negligibly small (ε and φ). This implies that the hot gas is optically thin and as a consequence, negligibly small radiation energy is absorbed by the hot gas.

(c) The temperature of the probe never reaches near that of the hot gas temperature. Radiation energy from the probe to the surroundings can be neglected.

Therefore, the radiation heat transfer from the probe to the surroundings can be neglected (See Section 2-3).

As shown in Section 2-4, if the ratio of diameter to

length of the leads is much less than unity, the conduction from the probe to the base of the leads can be neglected (See also Section 4-3 as well as References 5 and 6).

In the absence of radiation and conduction heat transfer, Equation (2) becomes

$$Q_s = Q_c \tag{7}$$

Therefore, convective heat is the only dominating means of energy transfer.

The oscillating probe response shown in Figure 4(b) contains heating and cooling curves resulting from convection to and from the probe. In Equation (3) it has been assumed that Q_c is a linear function of $(T_1 - T_2)$ or $(T_3 - T_2)$ as the case may be. The bead properties ρ_b and C_{pb} are assumed to be constant over the range of bead temperature variation.

During the heating part of the cycle, Equation (7) can be written as

$$\frac{dq}{dt} = Q_s = h_m A_b (T_1 - T_2) \tag{8}$$

where Q_s is given by Equation (6).
Using the boundary condition that $T_2 = T_o$ at $t = 0$, Equation (8) can be integrated to

$$T_2 = T_1 - (T_1 - T_o) e^{-\alpha_m t} \tag{9}$$

where

$$\alpha_m = (h_m A_b)/(\rho_b C_{pb} V_b)$$

During the cooling part of the cycle, Equation (7) can be written as

$$\frac{dq}{dt} = Q_s = h_o A_b (T_3 - T_2) \tag{10}$$

Now using the boundary condition that $T_2 = T_m$ at $t = 0$

Equation (10) can be integrated to

$$T_2 = T_3 + (T_m - T_3)e^{-\alpha_o t} \qquad (11)$$

where

$$\alpha_o = (h_o A_b)/(\rho_b C_{pb} V_b)$$

At $t = a$, $T_2 = T_m$ and Equation (9) becomes

$$T_m = T_1 - (T_1 - T_o)e^{-\alpha_o a} \qquad (12)$$

At $t = b$, $T_2 = T_o$ and Equation (11) becomes

$$T_o = T_3 + (T_m - T_3)e^{-\alpha_o b} \qquad (13)$$

Solving Equations (12) and (13) for T_o and T_m,

$$T_o = \frac{T_1(e^{-\alpha_o b} - e^{-\alpha_o b - \alpha_m a}) - T_3(1 - e^{-\alpha_o b})}{1 - e^{-\alpha_o a - \alpha_m b}} \qquad (14)$$

$$T_m = \frac{T_3(e^{-\alpha_m a} - e^{-\alpha_m a - \alpha_o b}) - T_1(1 - e^{-\alpha_m a})}{1 - e^{-\alpha_m a - \alpha_o b}} \qquad (15)$$

The mean thermocouple temperature is defined as

$$\bar{T}_2 = \frac{1}{2}(T_o + T_m) \qquad (16)$$

Inserting Equations (14) and (15) into (16)

$$(T_1 - T_3) = (\bar{T}_2 - T_3)\frac{2(e^{\alpha_m a + \alpha_o b} - 1)}{(e^{\alpha_m a + \alpha_o b} - e^{\alpha_o b} + e^{\alpha_m a} - 1)} \qquad (17)$$

The exponential terms, may be expanded using the following infinite series. $e^z = 1 + z + \frac{z^2}{2!} + \cdots\cdots$

Equation (17) becomes

$$(T_1 - T_3) = 2(\bar{T}_2 - T_3)[\alpha_m a + \alpha_o b + \text{2nd and higher order terms}] / [1 + \alpha_m a + \alpha_o b + \text{2nd and higher order terms} - 1 - \alpha_o b - \text{2nd and higher order terms} + 1 + \alpha_m a + \text{2nd and higher order terms} - 1] \qquad (18)$$

The second and higher order terms are $\left[\frac{1}{2!}(\alpha_m a)^2 + \frac{1}{3!}(\alpha_m a)^3 + \cdots\right]\left[\frac{(\alpha_o b)^2}{2!} + \frac{(\alpha_o b)^3}{3!} + \cdots\right]$, and, $\left[\frac{1}{2!}(\alpha_m a + \alpha_o b)^2 + \frac{1}{3!}(\alpha_m a + \alpha_o b)^3 + \cdots\right]$. They are now neglected since the terms $\alpha_m a = (h_m A_b a)/(\rho_b V_b C_b)$

and $\alpha_o b = (h_o A_b a)/(\rho_b V_b C_b)$

are always much less than unity. This may be shown to be so by means of an order of magnitude estimate as follows:*

$h_m = 3.5 \times 10^{-2}$ cal-cm^{-2}-sec^{-1}-$^{\circ}$K^{-1} (Section 2-3)

$C_b = 0.67$ cal-gm^{-1}-$^{\circ}$K^{-1}

$\rho_b = 8.6$ gm-cm^{-3} (See Reference 9)

$A_b = 8 \times 10^{-2}$ cm^2

$V_b = 2 \times 10^{-3}$ cm^3

then $\alpha_m = 0.23$ sec^{-1}.

Since the largest value of a is 0.1 sec.

therefore $\alpha_m a = 0.023$ which is very small and the second and higher powers of this term can be neglected.

The free convective heat transfer coefficient h_o from the probe in the water-cooled jacket can be expressed as:

$$\frac{h_o D_b}{K_f} = Nu_f = C(Gr_f\ Pr_f)^m \qquad \text{(Reference 9)}$$

The highest tempearture of T_o is 600 $^{\circ}$K, and, $T_3 = 290\ ^{\circ}$K,

$K_f = 1.3 \times 10^{-4}$ cal-cm^{-1}-sec^{-1}-$^{\circ}$K^{-1}

$Pr_f = 0.7$ (Reference 9)

$$Gr_f = \frac{g\beta_f (T_o - T_3) D_b^3}{\nu_f^2}$$

*For the theoretical estimates of this chapter c.g.s. units are used throughout. The experimental results referred to in Chapters 3 and 4 are all given in FPS engineering units.

$$g = 9.8 \times 10^2 \text{ cm/sec}^2$$

$$\beta_f = (\rho_3 - \rho_f)/[\rho_f (T_o - T_3)]$$

Under one atmosphere, $\rho_f \doteq \frac{1}{2}\rho_3$

then $\beta_f = 3 \times 10^{-3} \,^\circ\text{K}^{-1}$

$$\nu_f = 75 \times 10^{-2} \text{ cm-sec}^{-1}$$

$$Gr_f = 6$$

$$Gr_f Pr_f = 4.2$$

From Reference 9 page 166, Figure 7-8,

$$Nu_f = 1.2$$

then $h_o = 1.0 \times 10^{-3}$ cal-sec^{-1}-cm^{-2}-$^\circ$K^{-1}

The largest value of b is 1.6 sec.

Therefore $\alpha_o b = 0.011$

which is very small. The 2nd and higher power of this term and $(\alpha_o b + \alpha_m a)$ can be neglected.

As a consequence of neglecting second and higher order terms, Equation (18) becomes

$$(T_1 - T_3) = (\bar{T}_2 - T_3)(\alpha_m a + \alpha_o b)/\alpha_m a \qquad (19)$$

Introducing $H = \alpha_o/\alpha_m$, $R = b/a$

$$\theta_1 = (T_1 - T_3), \quad \bar{\theta}_2 = (\bar{T}_2 - T_3)$$

Equation (19) takes the form

$$\theta_1 = \bar{\theta}_2 (1 + HR) \qquad (20)$$

which will be used to evaluate the plasma temperature.

2.2 Utilization of Probe Heat Transfer Relation to Predict Hot Gas Temperature

It is extremely difficult to determine an accurate value for H. This is obvious from the difficulties even in obtaining the estimates of h_o and h_m made in Section 2.1. However, using two different cycling ratios R, one can eliminate H and obtain another equation to evaluate plasma temperature.

Changing only the cycling ratio from R to R', while keeping all other parameters constant, one obtains a new $\bar{\theta}_2'$ given by

$$\theta_1 = \bar{\theta}_2'(1 + HR') \tag{21}$$

Eliminate H from Equations (20) and (21)

$$\theta_1 = \bar{\theta}_2' + \frac{\bar{\theta}_2 - \bar{\theta}_2'}{1 - \frac{\bar{\theta}_2 R}{\bar{\theta}_2' R'}} \tag{22}$$

Since $T_1 = \theta_1 + T_3$, the hot gas temperature is known.

As a check on the accuracy of this method, a third value of R may be used. The combination of any two of these three sets of readings allows three calculations of hot gas temperature which should agree closely.

2.3 Radiation Correction

Raezer, Olsen and Henry considered the radiation heat lost by the probe through the hot gas to the surroundings to be negligibly small. The walls of the laboratory around the hot gas are the surroundings. Since in operation the probe temperature is always much less than that of the hot gas, radiation heat loss is small and can be neglected. Furthermore, the hot gas is assumed to be optically thin;

that is none of the radiation energy emitted by the probe is absorbed by the hot gas. The hot gas is assumed to be clean; that is, it does not contain suspended particles which could emit energy (10). In Reference 9, one can see that, the radiation energy emitted by an argon plasma at temperatures less than 5000°C is less than 10^{-5} of the net power of the arc jet. This too confirms the assumption of very little radiation heat transfer from the plasma.

An estimate is next made to calculate the magnitude of any radiation heat loss from the probe.

The surface heat transfer coefficient of the probe h_m, can be expressed as

$$h_m = \frac{Nu_a K_a}{D_b} \tag{23}$$

The Nusselt Number Nu_a of the hot gas may be determined from an expression given by Kramer and quoted by Hinze (11),

$$Nu_a = 0.42Pr_a^{0.2} + 0.57Pr_a^{0.33}\ Re^{0.5} \tag{24}$$

This expression holds good for $0.01 < Re < 10^4$.

In order to estimate the radiation heat loss, some value of the hot gas temperature and the corresponding T_m of the probe as well as other hot gas and probe properties must first be estimated. That is, it is necessary first to evaluate Re, Pr_a, Nu_a, h_o and h_m. Radiation heat loss would be largest at the maximum probe temperature. Values for the parameters C_{pa}, ρ_a, K_a, μ_a etc., are taken from References 9, 12 and 13. Referring to Figure 7(a), at any point in the flow path, it is assumed that the ideal gas relationship can be used to relate

P, F and T.

Therefore $P_4 F_4 \propto T_4$

$P_5 F_5 \propto T_5$ (T_5 = 6000°K, an estimated value according to Figure 14)

then $P_5 F_5 = \frac{T_5}{T_4} P_4 F_4$

$F_5 = 1080 \text{ cm}^3\text{-sec}^{-1}$

$U_5 = 1.4 \times 10^5 \text{ cm-sec}^{-1}$

$a_5 = 1.55 \times 10^5 \text{ cm-sec}^{-1}$ (Reference 13, pp. 129)

Therefore $M_5 = 0.9$

At the point $T_1 = 2500°K$, the maximum probe temperature $T_m = 1100°K$. The velocity at that point is estimated as follows:

$F_1 = 450 \text{ cm}^3\text{-sec}^{-1}$

$U_1 = 6 \times 10^4 \text{ cm-sec}^{-1}$

Reynolds Number at Point 1 is defined as

$$Re = \frac{U_1 D_b \rho_a}{\mu_a}$$

where $\rho_a = 2.1 \times 10^{-4} \text{ gm-cm}^{-3}$

$\mu_a = 1 \times 10^{-3} \text{ gm-cm}^{-1}\text{-sec}^{-1}$

then $Re = 2 \times 10^3$

Prandtl Number at Point 1 is defined as

$$Pr_a = \frac{C_{pa} \mu_a}{K_a}$$

where $C_{pa} = 0.16 \text{ cal-gm}^{-1}\text{-}°K^{-1}$

$K_a = 2.5 \times 10^{-4} \text{ cal-cm}^{-1}\text{-sec}^{-1}\text{-}°K^{-1}$

then $Pr_a = 0.64$

Substitute the values of Re and Pr_a into Equation (24) then

$Nu_a = 22.2$

The heat transfer coefficient h_m is

$$h_m = 3.5 \times 10^{-2} \text{ cal-cm}^{-2}\text{-sec}^{-1}\text{-}^{\circ}\text{K}^{-1}$$

Convective heat transfer from the hot gas to the probe is estimated as $Q_c = h_m A_b(T_1 - T_m)$

Therefore $Q_c = 4.6 \text{ cal-sec}^{-1}$

Radiation heat transfer from the probe to the surroundings is expressed in Equation (5) as:

$$Q_r = \sigma \epsilon_b A_b T_m^4 - \sigma \alpha_b A_b T_r^4 \quad \text{(Reference 10)}$$

The second term is much less than the first term, therefore it is neglected in the following calculation.

$$Q_r = \sigma \epsilon_b A_b T_m^4$$

$\epsilon_b = 0.7$ (Reference 13)

$\sigma = 1.34 \times 10^{-12} \text{ cal-sec}^{-1}\text{-cm}^{-2}\text{-}^{\circ}\text{K}^{-4}$

then $Q_r = 1.1 \times 10^{-1} \text{ cal-sec}^{-1}$

Therefore the ratio

$$\frac{Q_r}{Q_c} = 2.4 \times 10^{-2} \ll 1$$

is negligibly small.

Consequently one can see that radiation heat lost by the probe to the surroundings is in fact negligible. At lower T_1 and T_m, radiation loss would be even less.

2.4 Conduction Heat Loss Along the Leads

Raezer and Olson neglected the conduction along the leads of the probe in his high-power atmospheric argon plasma jet

tempearture measurement. However, Henry (5) found that in his vacuum chamber, conduction along the leads was significant. Raezer supported his assumption on the basis that the ratio between the area and length of the leads was far less than unity. However, Henry theoretically evaluated the conduction with the condition that the probe tip was in free-molecular flow.

In this experiment, the probe is in continuum flow at one atmosphere pressure. The approximate value of conduction is calculated below and compared with the estimated convection.

The expression for heat conduction along the leads is estimated as

$$Q_k = \frac{2\ K_w\ A_w}{L_w}\ (T_m - T_{wb})$$

where thermal conductivity of the leads K_w is

$$K_w = 5 \times 10^{-2}\ \text{cal-sec}^{-1}\text{-cm}^{-1}\text{-}^{\circ}\text{K}^{-1} \quad \text{(Reference 14)}$$

diameter of the leads

$$D_w = 0.02\ \text{cm.}$$

length of the leads

$$L_w = 0.25\ \text{cm.}$$

then

$$\frac{D_w}{L_w} \leq 0.1$$

is much less than unity.

$T_m = 1100\ ^{\circ}\text{K}, \qquad T_{wb} = 500\ ^{\circ}\text{K}$

Therefore, $\quad Q_k = 7.50 \times 10^{-2}\ \text{cal-sec}^{-1}$

and the ratio

$$\frac{Q_k}{Q_c} < 2.0 \times 10^{-2}$$

is negligibly small.

One can see that during the heat transfer from the hot gas flow to the probe under one atmosphere pressure with $D_w / L_w < 0.1$, convection is the dominating means of energy transfer.

3. EXPERIMENT

3.1 Apparatus

The experimental apparatus consists of a chromel-alumel subminiature thermocouple of 1/16 inch sheath diameter, 12 inches long. A low-power plasma jet generated the argon plasma. A water-cooled jacket with a double acting solenoid was mounted around the sheath of the probe. An electronic timing circuit supplied a square-wave current to the double acting solenoid in order to push and pull the probe in and out of the plasma. Two storage batteries in series were used to supply 24 volt D.C. power to both the timing circuit and the solenoid. Argon gas was used as the plasma-jet working fluid. Honeywell Accudata 120 D.C. and 117 D.C. amplifiers, along with a Honeywell Visicorder, were used to record the response of the probe and the frequency of the square-wave current. A Textronex Type 564 Storage Oscilloscope with Type 3A3 Amplifier was used to record the magnitudes of times "a" and "b" of each probe pulse. A Miller model 330 A/BP AC-DC inert gas welder supplied power to the arc jet. Figures 5 to 10 show the experimental set-up.

3.2 The Choice of the Working Fluid

The choice of the fluid depended on the best compromise -

between the following requirements (15).

(a) Low ionization energy.

(b) Non corrosive---- a clean gas.

(c) The ionization potential and electrical conductivity should permit the establishment of a stable arc column.

Helium and argon are two of the inert gases that have the above properties. Argon is perhaps the most often used in plasma experiments, especially with arc jets. For this reason argon plasma properties are perhaps best known and most fully tabulated. Besides, experience has shown that arc-jet lifetime is considerably greater when argon is used. Helium has a habit of causing very unstable arc operation and premature electrode burn-out. Therefore, argon was chosen as the working fluid.

3.3 The Design of the Arc Jet (Figure 10)

The arc jet was designed to operate under atmospheric pressure. Argon from the cylinder passed through the pressure regulator and then to the arc jet. In the arc jet, the argon was spiralled through two helical slots forming a swirling vortex and then injected tangentially at the periphery of the arc chamber to stabilize the

arc column.

This rotating motion of the injected fluid has multiple advantages (15).

(a) It can centrifugally constrain the hot gas discharge column to the axis of the vortex.

(b) It can prevent the arc column from sticking at one point on the electrode causing its sudden destruction.

(c) It can cool the electrode and chamber walls..

(d) It can bring the gas into better and longer contact with the arc column, thereby heating the gas to a higher temperature.

The arc jet was designed so that the center electrode could be moved axially, even while in operation, by turning the plexiglas flanges (Figure 11). The complete arc jet was mounted on a special traversing table which had adjustment for both lateral and axial motion. Both the anode and cathode were water-cooled as shown in Figure 11.

3.4 Instrumentation

A variable frequency signal was provided by a multivibrator circuit with variable delay time through a high current semiconductor rectifier switching circuit to control the solenoid current. This current, through the

double-acting solenoid, was used to drive the probe in to and out of the plasma. The timing rate was adjusted with regard to the plasma temperature, thermal conductivity and thermal capacity of the probe. Therefore, the cycling rate $R = b/a$ was selected on the basis of the different specific conditions. At lower plasma temperature, R could be smaller , however, at higher temperature R had to be larger. The magnitude of R was limited by the time constant available with the multivibrator circuit and also by the inertia of the probe moving in to and out of the water-cooled jacket. In this experiment R was varied between 1 to 20. The pulse widths "a" and "b" of the flip-flop current were recorded by feeding the signal through a Honeywell Accudata 117 D.C. amplifier to another channel of the Honeywell Visicorder (See Figure 8).

The pulse widths of the probe response were also displayed on an oscilloscope. A comparision of pulse widths obtained in these two ways showed little difference between them. For the sake of accuracy, the pulse widths obtained from the oscilloscope were used for "a" and "b" in calculating the cycling ratio R.

Ideally, the travelling time of the probe passing from one reservour to the other should be zero. In the experiment the travelling time should be negligibly small compared to "a" and "b". In order to do this, the inertia of the probe has to be very small, meaning that the probe

must be light and have little frictional resistance to its motion.

The temperature T_3 of the cold reservoir was taken as the temperature of the probe when it was sitting still in the water-cooled jacket for a period of time long enough for the probe to reach a steady temperature. This temperature was displayed on an oscilloscope.

The power to the arc jet was provided by a Miller welder capable of supplying 50 to 250 amperes D.C. continuously. A voltmeter and an ammeter indicated the voltage drop and current flow through the arc jet. A flow-meter mounted on the argon gas cylinder indicated the flow rate in cuft/hr*.

3.5 The Choice of the Thermocouples

Chromel-alumel subminiature thermocouples made by Thermo Electric (Canada) Limited were chosen for this experimental investigation for the following reasons:

(a) This type has a high melting point.

(b) They have high tensile strength to withstand sudden acceleration.

Though other thermocouples such as platinum-platinum 10% rhodium have higher melting points than chromel-alumel,

---

* Flow rates quoted are those measured by the gauge on the gas bottle and are at 4.45 atm., and room temperature.

they lack the tensile strength to withstand sudden acceleration.

The exposed loop type of measuring junction was used. Other types of measuring junctions such as grounded type and insulated junction type are shown in Figure 5. The exposed loop type is better than others for the following reasons:

(a) The volume of the sensing part is small, only the small bead touches the hot plasma, therefore, the local temperature measurement can be obtained at the point of interest.

(b) Since the area of the sensing part is small, radiation correction is negligibly small.

(c) No significant conduction heat loss through the leads as there would be through the sheath.

3.6 Thermocouple Calibration

The signal from the thermocouple probe was fed through a Honeywell Accudata 120 D.C. amplifier and then to a Honeywell Visicorder for recording. A typical output can be seen in Figure 12.

A standard known voltage signal from a potentiometer was used to calibrate the amplifier and recorder system. A calibration table for chromel-alumel thermocouples was used to determine the probe temperature. The reference temperature of this table was 25°C. The room temperature which varied

from 22°C to 28°C was taken as the cold junction temperature of the probe, since the difference between the 25°C reference temperature of the table and room temperature was very small compared with the probe temperature.

3.7 Experimental Procedure

Equation (22)

$$\theta_1 = \bar{\theta}_2' + \frac{\bar{\theta}_2 - \bar{\theta}_2'}{1 - \frac{\bar{\theta}_2 R}{\bar{\theta}_2' R'}}$$

showed that, the hot gas temperature θ_1 could be determined by using two different values of R which results in two different values of thermocouple mean temperature at the same specific conditions (gas flow rate, arc current, voltage of the electrode and distance along the axis of the arc jet). With a third value of R, a third different mean temperature $\bar{\theta}_2$ could be obtained at the same condition. By taking the three results, two at a time, it was possible to obtain, using Equation (22), three values of the hot gas temperature at the point of interest. If they differed from each other by less than 5%, the average of these three values was accepted as the temperature of the hot gas at these specific conditions (See Section 4-1 for further discussion of this deviation).

Now $R = b/a, \quad R' = b'/a'$

$R'/R = (b'/a') \times (a/b)$

If "a" was fixed in each "R", then, Equation (22) can be written as

$$\theta_1 = \bar{\theta}_2' + \frac{\bar{\theta}_2 - \bar{\theta}_2'}{1 - \frac{\bar{\theta}_2 b}{\bar{\theta}_2' b'}} \qquad (37)$$

Fixing three values of "b" by inserting three fixed resistors into the vibrator circuit, one can easily switch from one "R" to another "R" maintaining "a" constant.

Temperature measurements were made along the axis of the jet from $\frac{1}{2}$ to 4 inches from the nozzle face (Figures 13 to 18). A few points were taken 0.0885 inch off the axis of the jet (Figures 19 and 20). Readings were made at a number of different gas flow rates, arc currents and distances along the axis. At each condition, after steady and smooth operation had been obtaioed, three readings were taken using three different values of R (Figure 12). At each cycling rate, 60 seconds were allowed for the probe operation to reach a steady state and then traces were recorded for a further 10 seconds. A serious problem occasionally encountered was that the arc jet would flicker, changing the plasma temperature during the time necessary to obtain the three 10-second traces. Readings had often to be repeated if the three values of

plasma temperature calculated from the three different cycling rates at the same point and conditions differed by more than 5%.

The response of the probe depended mainly on the heat capacity of the bead as well as on the temperature of the plasma. Therefore, probes with different bead diameters were used in several tests. Results showed that for higher plasma temperature measurement, the larger bead was preferable (Refer to the discussion in section 4-3).

Several different methods were tried to increase the bead size. One was by the use of an oxygen-acetylene flame. In this way, oxidization of the material could not be avoided; also a spherical shape to the bead could not easily be obtained. The most sucessful method employed the continual use of the spark welder on the bead until sufficient material had built up in a spherical shape.

Temperature curves were taken with two different nozzle diameters 0.125 and 0.177 inch (Figures 13 to 15 and 16 to 20). Starting was accomplished by means of a high frequency starter on the welder and occasionally by also reducing the distance between the tungsten cathode and the jet nozzle. The distance between the cathode and nozzle was controlled by rotating the plexiglas flanges (See Figure 11). This distance was usually kept less than 3/16 inch to start the jet. During operation, the electrode spacing was usually adjusted to about

3/8 inch for most stable operation. For different flow rates, while using the 0.125 inch nozzle diameter, the voltage drop was approximately constant; but using the 0.177 inch nozzle diameter, the voltage drop increased approximately one volt for each 5 cuft/hr of gas flow rate.

Sometimes, during experiments, the probe would stick somewhere inside or outside of the water-cooled jacket. When inside the jacket, the jet was turned off, the solenoid checked, and then the circuit and probe was restarted. Outside, it was necessary to shut down the power before the bead burnt out. A remote control of the power source was always in hand.

3.8 Results

The temperature profiles along the axis of the 0.125 inch nozzle plasma jet obtained for each gas flow rate and arc current are shown in Figures 13, 14 and 15. Through comparison it may be seen that temperature is generally inversely proportional to gas flow rate, proportional to arc current and inversely proportional to the distance along the axis. Since the voltage was always nearly constant, power variation has the same variation as arc current. The inverse proportion between the temperature and gas flow rate is reasonable, since at fixed energy input, that is arc current constant, increasing the gas flow rate would decrease the energy added to each particle. Therefore the flow temperature is likely to be lower

at higher gas flow rates. The proportional relationship between the temperature and arc current is also reasonable since the current and voltage are the energy source to ionize the gas. At higher current flow, and fixed voltage, the energy of the particles is higher, resulting in higher gas temperature.

For this nozzle diameter, one dependent variable T_1 and three independent variables F (gas flow rate), I (arc current) and Dist (distance along the axis of jet) were used to set up a functional relationship of the form T = fn(F,I,Dist). Using a factorial plan method, these can be formed into an algebraic equation. The result, calculated from this algebraic equation described below, when compared to the experimental results, showed a deviation of less than 10%.

3.9 Factorial Plan

The independent variables were varied over the following ranges

Arc current: 75 to 150 amperes in increments of 25 amperes.

Gas flow rate: 10 to 20 cuft/hr in increments of 5 cuft/hr.

Positions from nozzle: 4, 3, 2, 1.5, 1, 0.875, 0.75, 0.625, 0.5 inch.

It is assumed that the temperature difference may be represented by the following equation

$$\Delta T = W I^a F^b (Dist)^c \tag{38}$$

where $\Delta T = T_1 - T_r$

T_r is the argon gas temperature before entering the jet.

W is an arbitrary constant.

a, b, c are constants to be determined.

Taking the logarithm of both sides,

$$\log \Delta T = \log W + a \times \log I + b \times \log F + c \times \log (Dist) \tag{39}$$

Keeping F(Dist), FI, ID constant one at a time, and differentiating:

$$\frac{d(\log \Delta T)}{d(\log I)} = a \tag{40}$$

$$\frac{d(\log \Delta T)}{d(\log F)} = b \tag{41}$$

$$\frac{d(\log \Delta T)}{d(\log Dist)} = c \tag{42}$$

In Figures 21 to 24 are plotted $\log \Delta T$ vs log I, $\log \Delta T$ vs log F, $\log \Delta T$ vs log (Dist) each with F(Dist), I(Dist), FI

constant respectively. The slopes a, b, c for each group are calculated averages.

Finally

$$\Delta T = W \times I^{0.87} \times F^{-0.38} \times (Dist)^{-1.18} \qquad (43)$$

W is determined by substituting one of the experimental data points T_1 into Equation (43).

Therefore

$$\Delta T = 30 \times I^{0.87} \times F^{-0.38} \times (Dist)^{-1.18} \qquad (44)$$

or

$$T_i = 30 \times I^{0.87} \times F^{-0.38} \times (Dist)^{-1.18} + T_r \qquad (45)$$

Using Equations (44) and (45), Figures 25 to 28 were plotted. Comparing these with Figures 13, 14, 15 and 21, it may be noted that Equation (45) describes the functional relationship within an error of less than 10%.

Temperature profiles obtained using the 0.177 inch jet diameter are shown in Figures 16 to 20. In this case, voltage changes were noted at the different gas flow rates. For each 5 cuft/hr increase of gas flow rate, voltage drop increased about one volt. This phenomenon is probably due to a decrease of plasma conductivity at increased gas flow rate (15). By inspection of Figures 16 to 18, it may be seen that at low arc current, the temperature profiles at low gas flow

rates are lower than those at high gas flow rates. This is the reverse of that obtained with the small jet nozzle. However, at high arc current, the situation is reversed again. Because of this phenomenon, it is not possible to apply the method of factorial plan to this data.

4. DISCUSSIONS AND CONCLUSION

4.1 Discussion of 5% Deviation

The temperature along the center line of the plasma jet was not always constant under fixed conditions, but would fluctuate frequently. At temperatures of 800°C, the fluctuation often amounted to around 30°C. At higher temperatures, it might be expected that the fluctuation would be greater. Due to this, it is to be expected some error will be present and thus a limit of 5 % deviation between the three calculated values of hot gas temperature is acceptable.

4.2 The Effect of Large Fluctuations of the Arc Jet

If some particles of "lava", tungsten or copper through ablation are injected into the hot gas, or if some inpurity exists in the argon gas, then the arc jet would flicker changing the plasma temperature. The plasma would fluctuate seriously or change to another stable state. In the first case, the arc jet had to be turned off and restarted. In the second case, if this changing of stable state was not detected in time, a wrong reading would sometimes result. Then, the calculated T_1 would be far away from the mean curve through the other points. This can be seen in Figures 13 to 20.

4.3 The Effect of Bead Diameter

The effect of the bead diameter can be seen as follows:

(a) The bead diameter can affect the radiation heat loss in the manner described below:

Radiation heat lost by the probe was estimated in Section 2-3 as:

$$Q_r = \sigma \epsilon_b A_b T_m^4$$

Here we see that this loss is directly proportional to the surface area of the bead. A larger bead would increase this loss. However in this experiment the larger bead, with a diameter of 0.063 inch, had an estimated radiation loss that was negligibly small.

(b) Probe Response.

Initially, when a small bead diameter was used it was found that output excursions were too great because the probe response was too fast. A limitation was imposed by the maximum cycling rate obtainable with the drive circuit. Later, bead size was increased to about 0.063 inch diameter with the result that the decreased probe response gave a more useful output.

The arc jet, although operating continuously for long periods of time with little wear and no appreciable

change in operating state did occasionally flicker with conditions fluctuating slightly. The larger bead size was less sensitive to these changes and consequently was better.

4.4 The Effect of Cycling Ratio R

One can see by Equation (22) that the range of hot gas temperature measurement depends on the cycling ratio "R" as well as "$\bar{T}_2$". Here "$\bar{T}_2$" is limited by the melting point of the thermocouple. Increasing the value of "R" could decrease "$\bar{T}_2$" (See Figure 12) when measuring the same temperature. Therefore, in order to evaluate higher hot gas temperatures, "R" should be higher.

4.5 Conclusion

In this experiment, a powerful and cheap tool was built and used to measure local atmospheric plasma temperatures up to 2600°K. The present research has proved the usefulness of this devise to predict local plasma temperature. The chromel-alumel probe with a bead diameter of 0.063 inch was found to give better results than a smaller diameter probe.

A rugged stable arc jet has been constructed to run at low power levels. The voltage drop between the electrodes has been found to be a function of electrode distance and gas flow rate. Using a 0.125 inch jet nozzle diameter, the

effect of gas flow rate on voltage drop was insignificant. As a result, it was possible to apply a factorial plan to analyse the results. However, with a 0.177 inch jet nozzle diameter this was not so, and it was impossible to apply a factorial plan to the data. If some operating adjustment is made to change the electrode spacing in order to keep the voltage drop constant for each gas flow rate, it might also be possible to analyse the 0.177 nozzle temperature characteristics by means of a factorial plan.

It is also suggested here that additional information about the plasma might be obtained from the same probe. This could be done by biasing the probe bead with a voltage and using it at the same time as one would a Langmuir probe. In this manner it might be possible to obtain electron temperature and charge density data as well as heavy particle temperature.

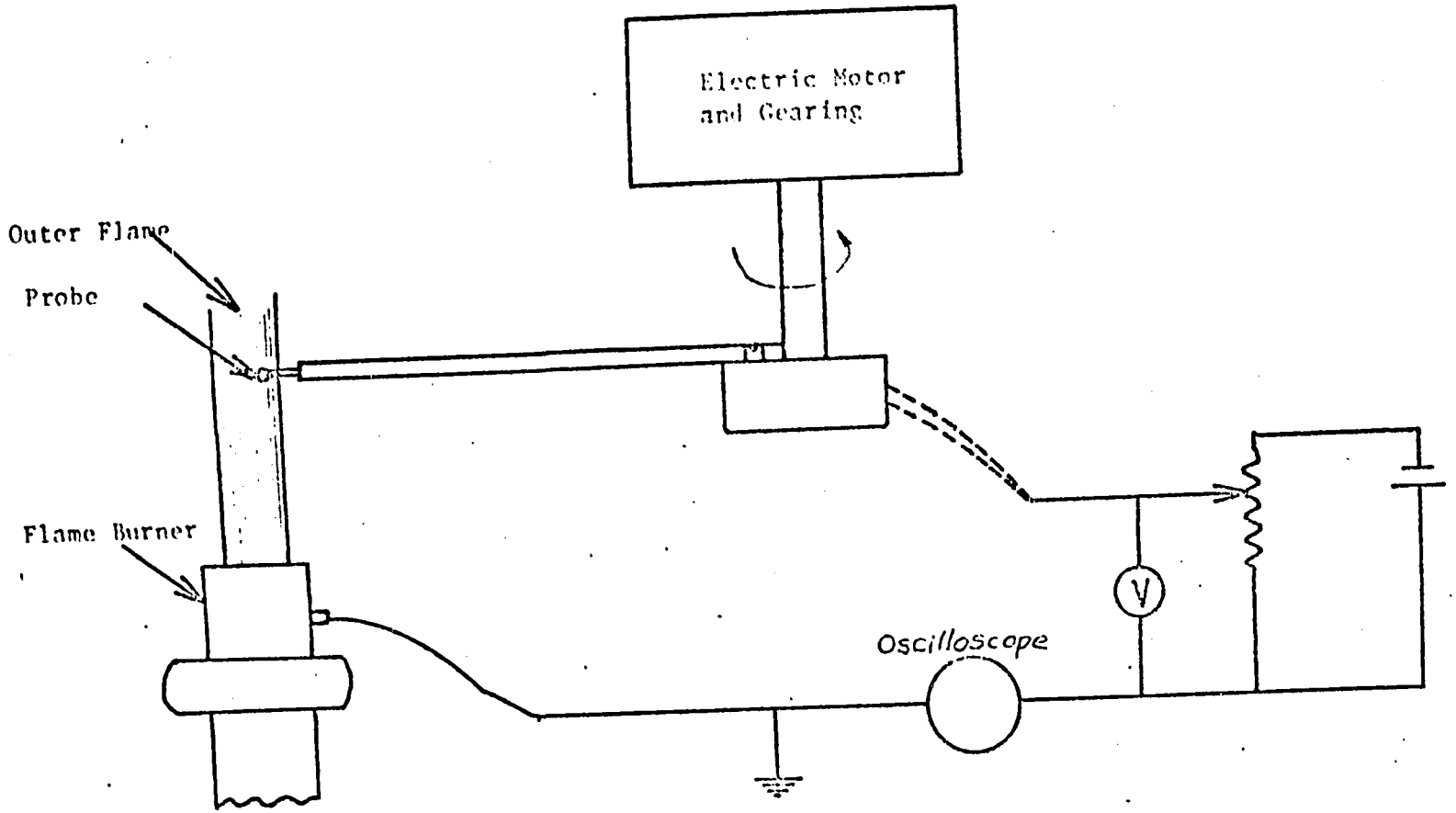

Figure 1: Electrostatic Probe Assembly.
(After Reference 1)

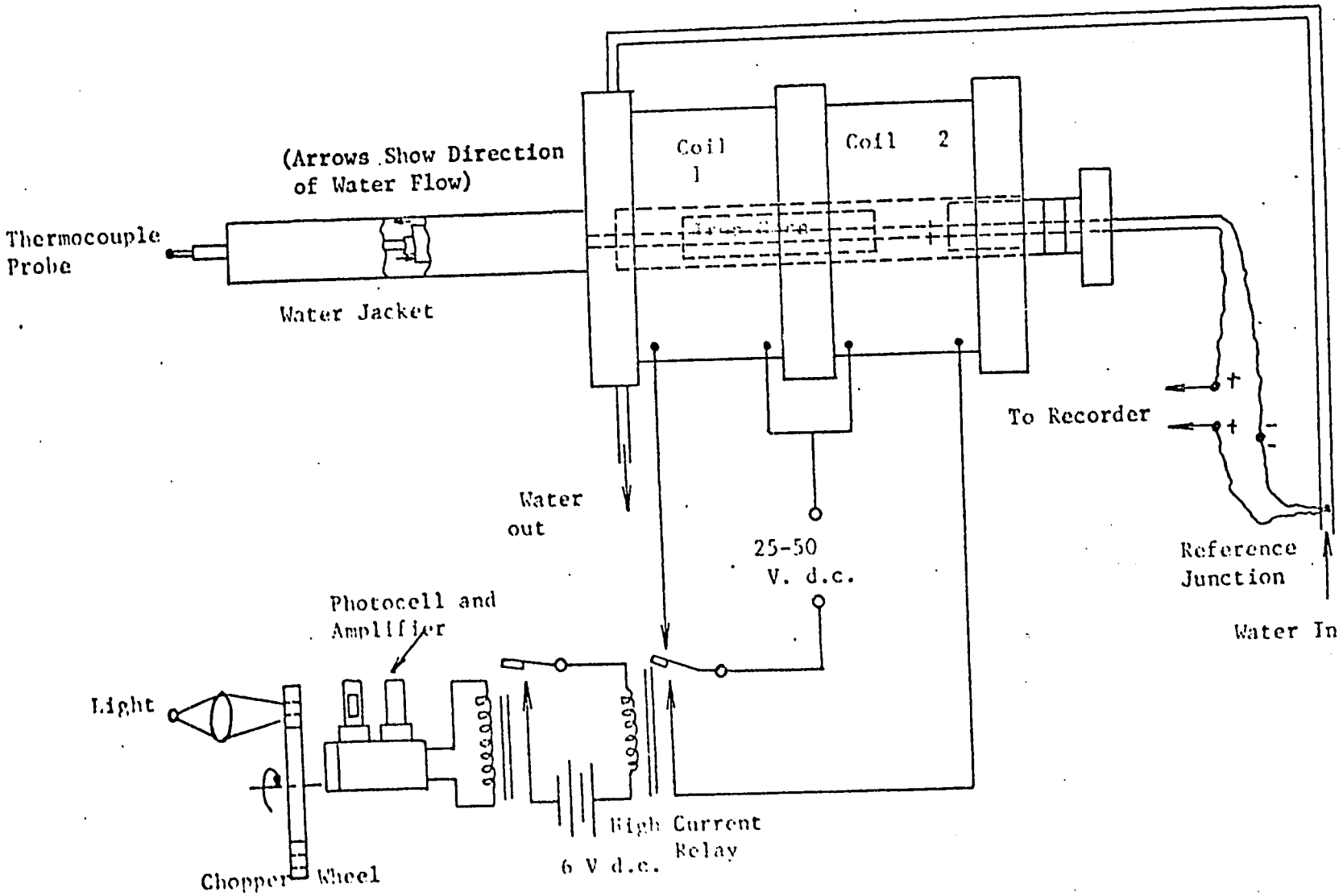

Figure 2: Intermittent Thermocouple and Cycling Circuit. (After Reference 5)

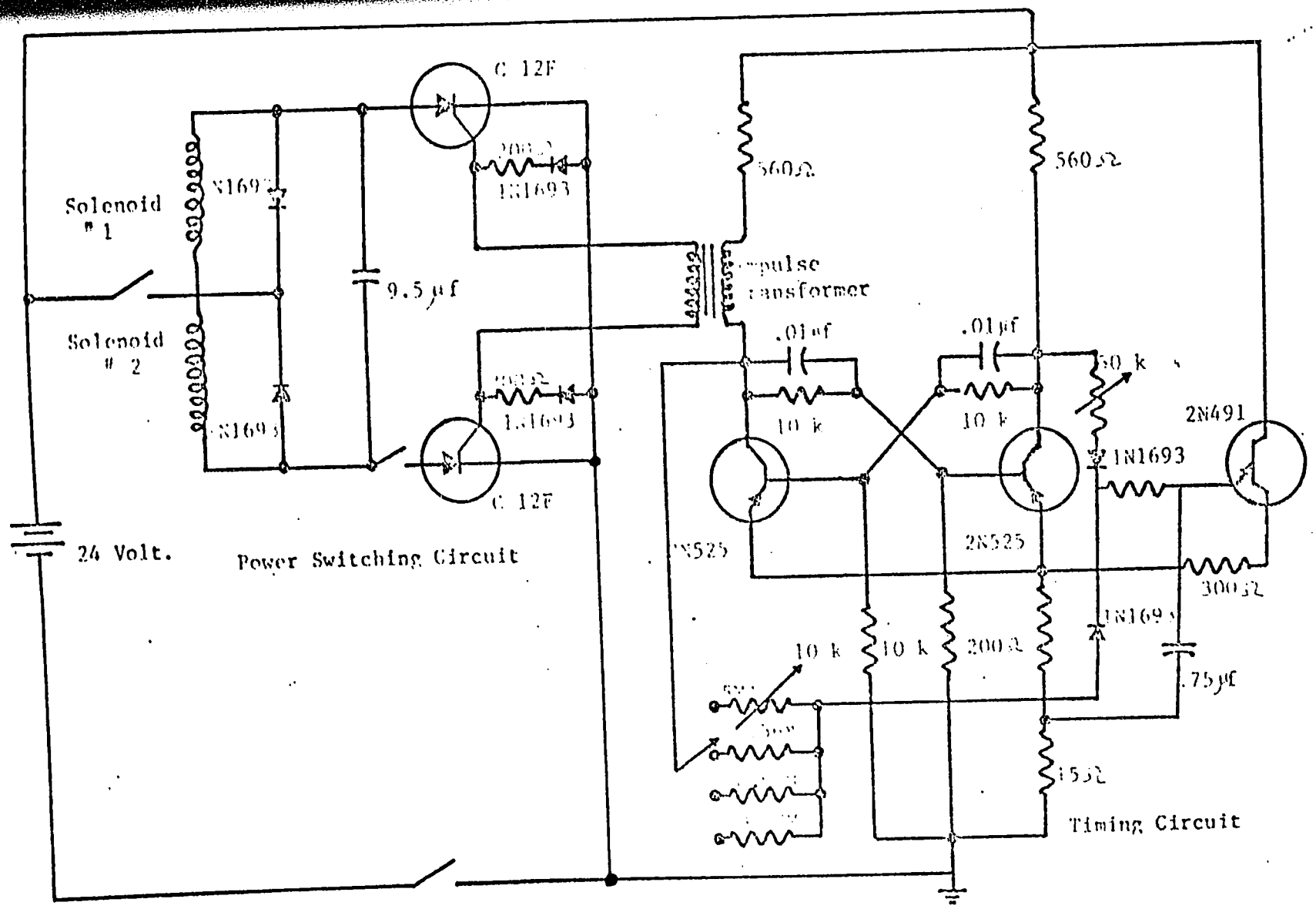

Figure 3: Schematic Diagram of the Probe Driving Circuit

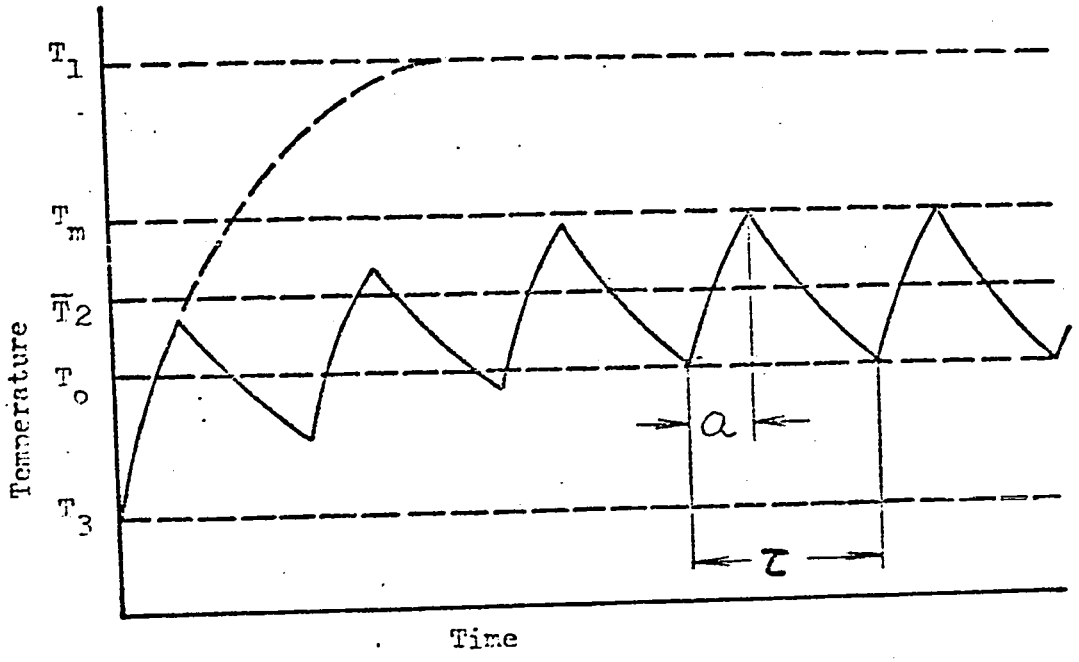

(a) Sketch of Time-Temperature Trace for Intermittent Thermocouple.

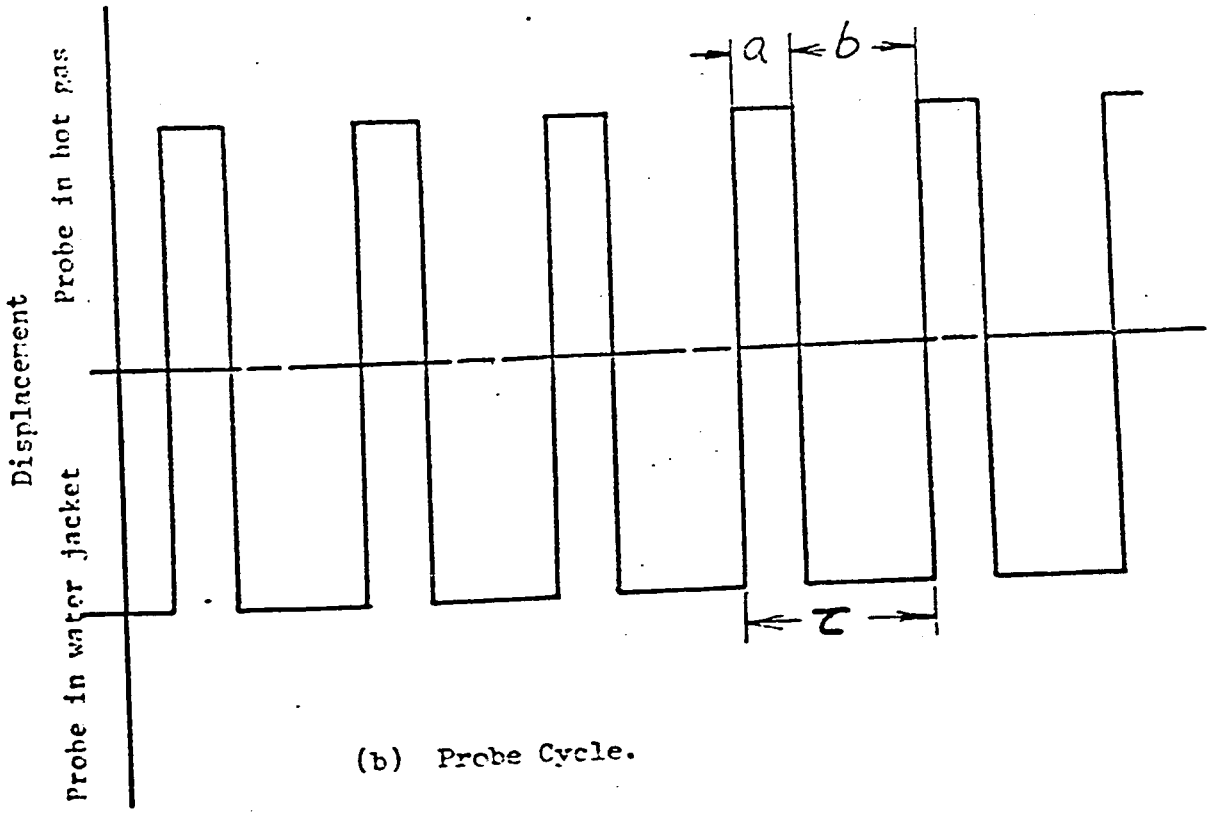

(b) Probe Cycle.

Figure 4:

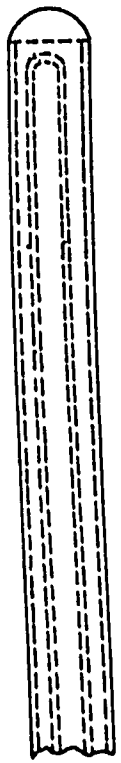

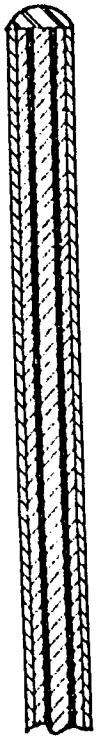

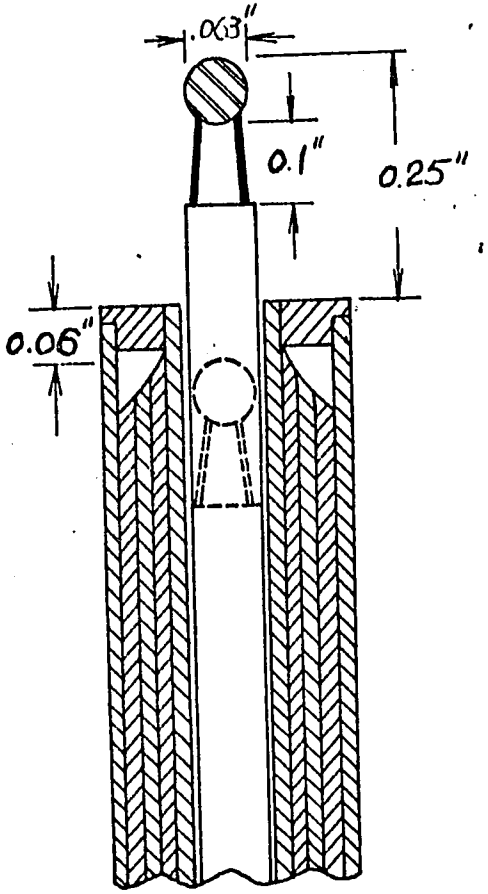

Sheath
Thermocouple Tip
Thermocouple Leads
Ceramic

Brass Tube
Bead
Thermocouple Leads

(a) Insulated Measuring Junction. (b) Grounded Measuring Junction. (c) Exposed Loop Measuring Junction.

Figure 5: Sketch of Different Types of Probe Junction

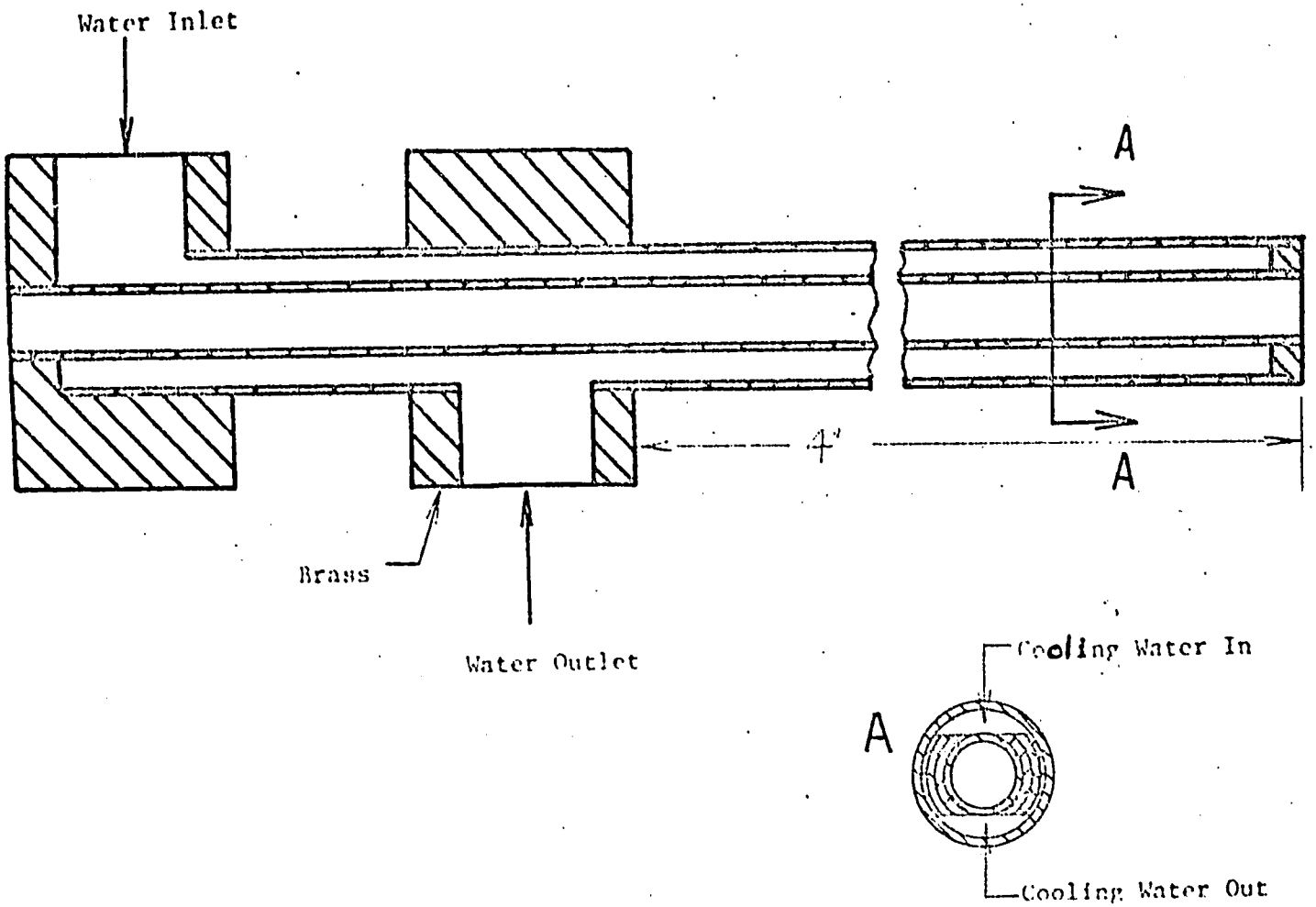

Scale 4:1

Figure 6: Design of Water-Cooled Jacket.

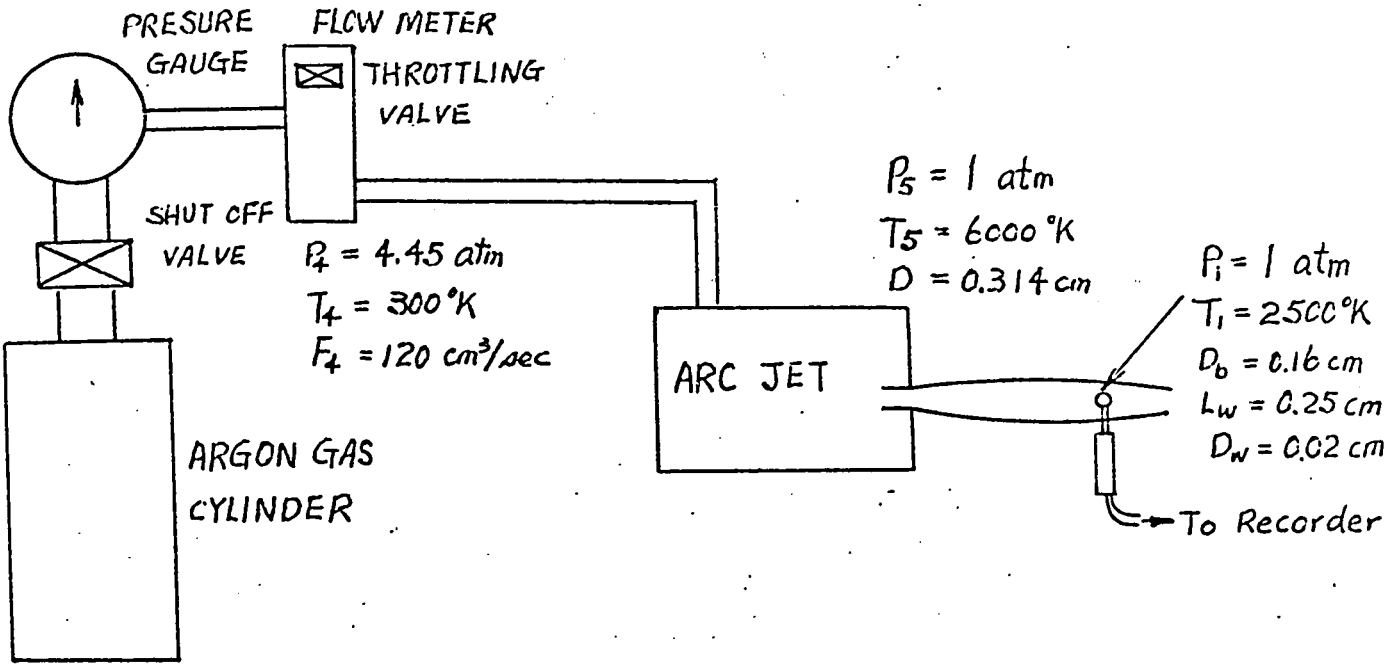

(a) Schematic Diagram of Gas Flow

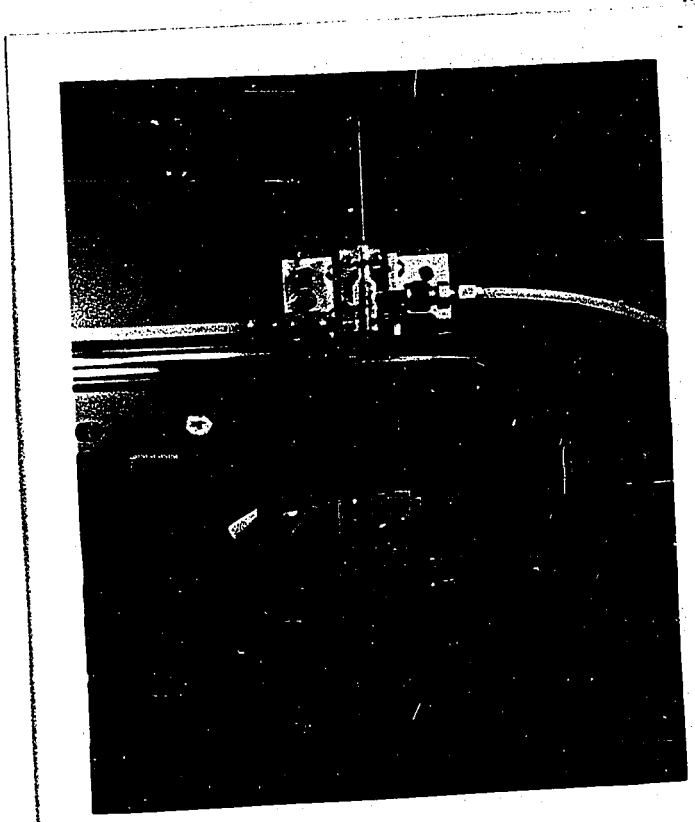

(b) General View of Water-Cooled Jacket and Double Acting Solenoid.

Figure 7

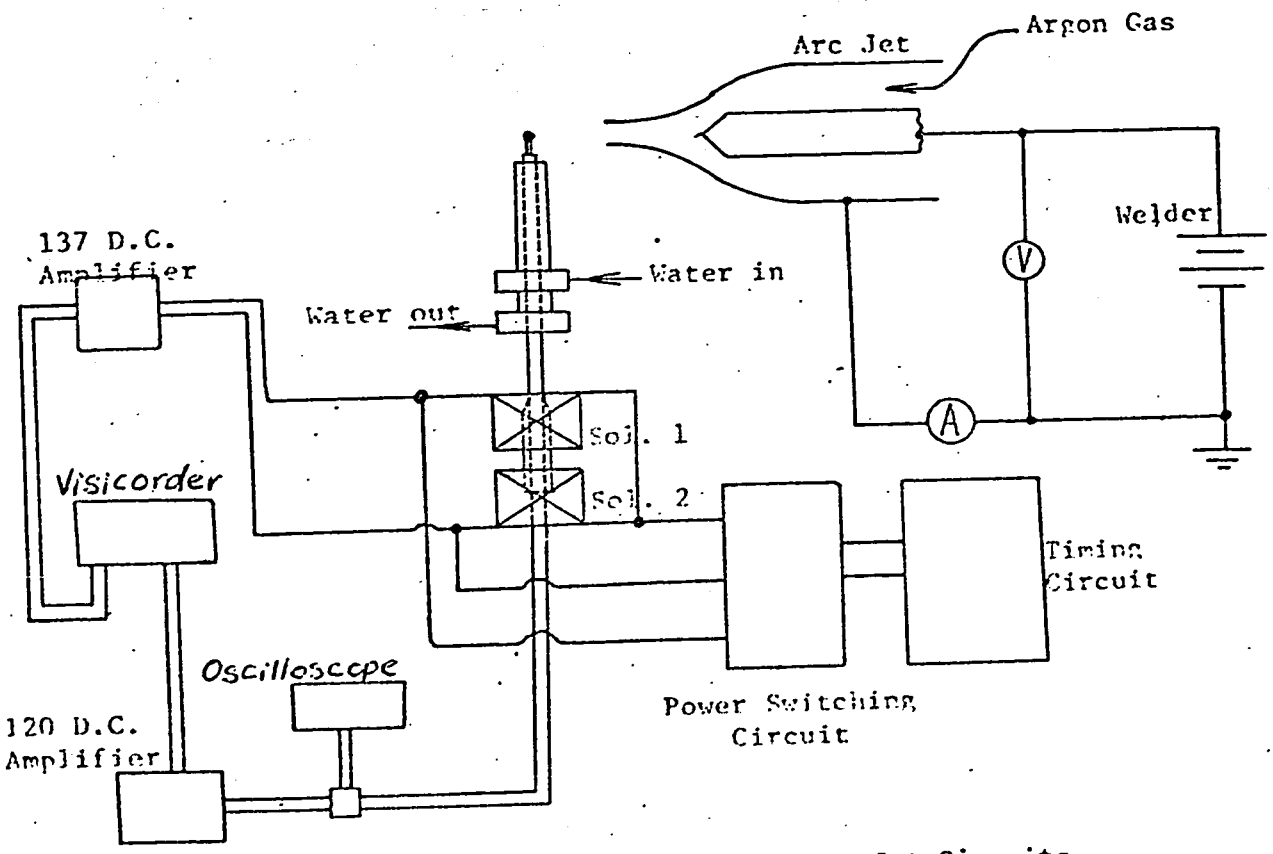

(a) *Schema* of Probe and Plasma-Jet Circuits.

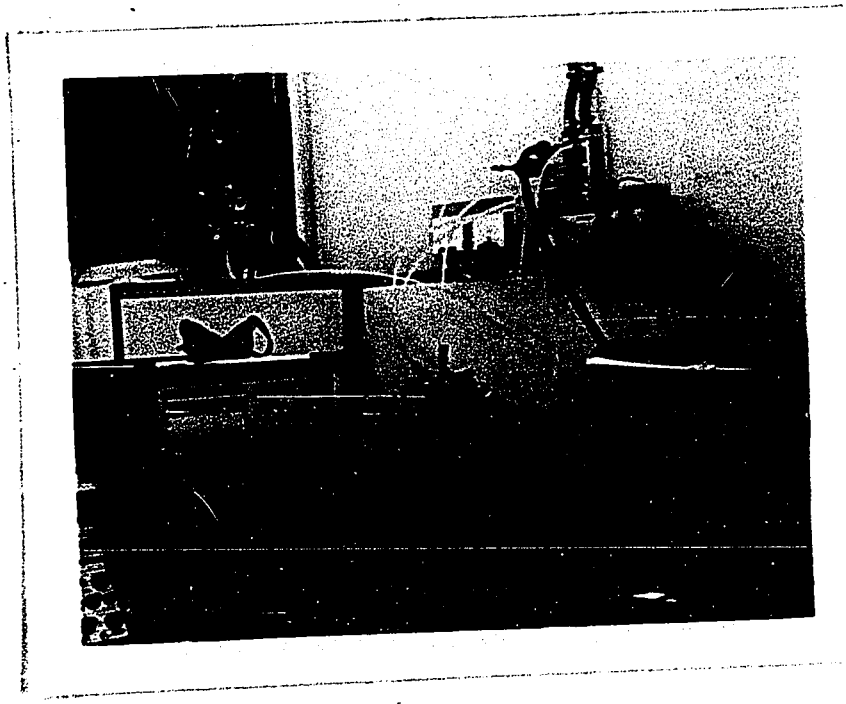

(b) Complete Experimental Apparatus.

Figure 8:

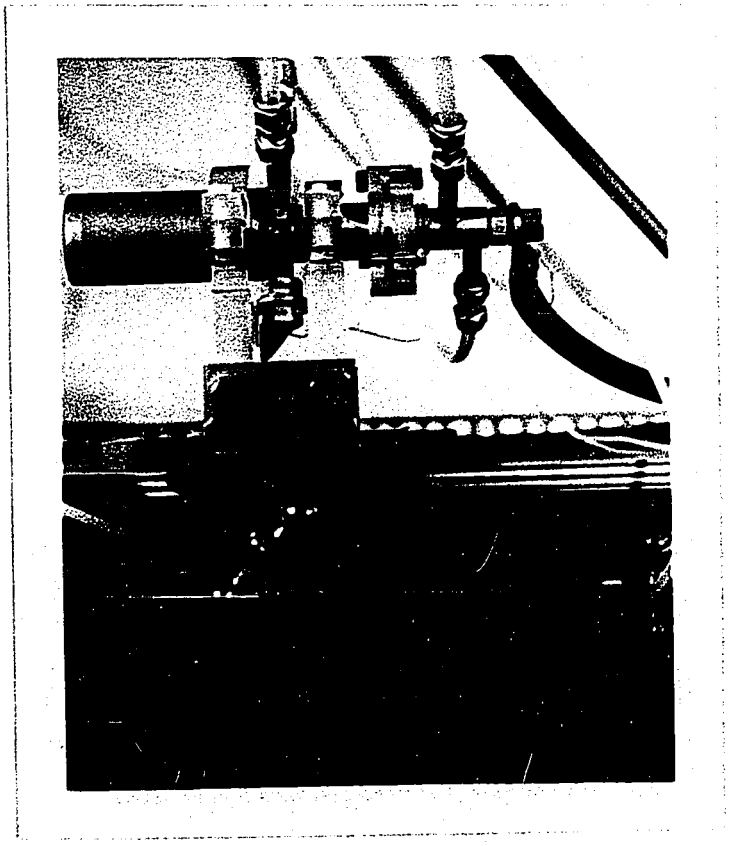

(a) General View of the Arc Jet Model.

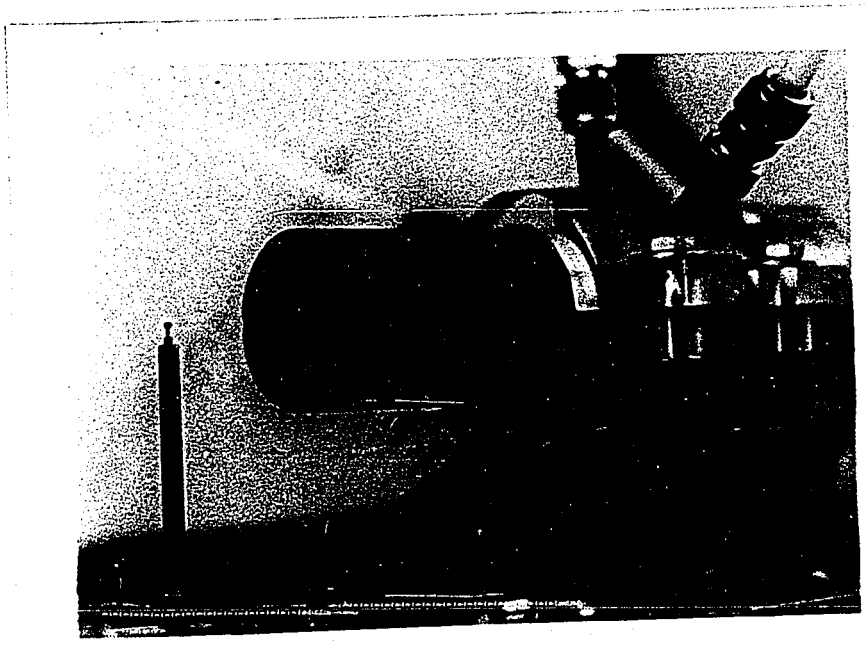

(b) Side View of the Probe and Jet.

Figure 9:

(a) 0.177 inch Jet Nozzle Diameter
20 cuft/hr Flow Rate
150 amp Arc Current

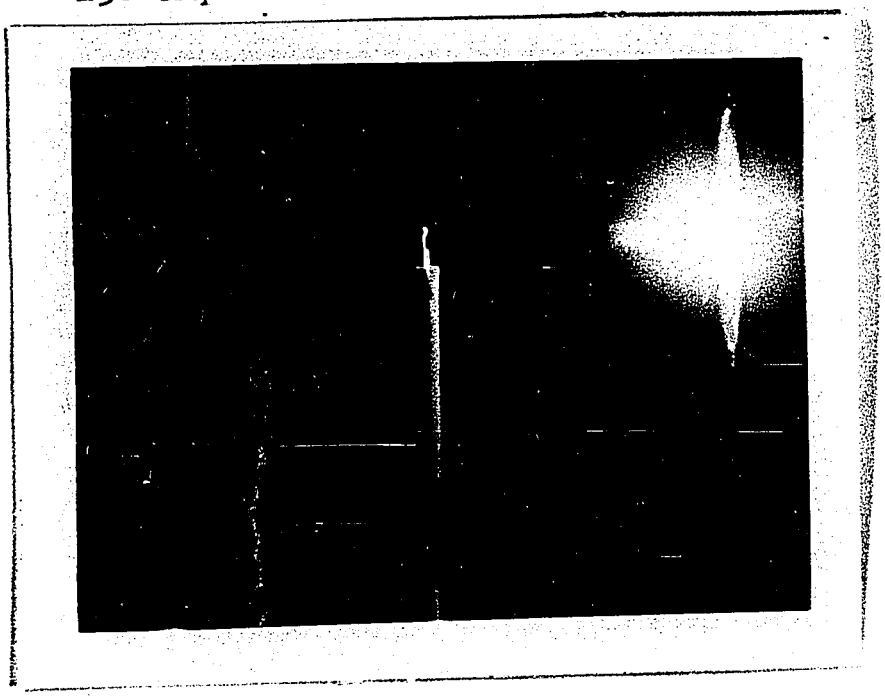

(b) 0.177 inch Jet Nozzle Diameter
15 cuft/hr Flow Rate
150 amp Arc Current

Figure 10: Photographs of Arc Jet in Operation

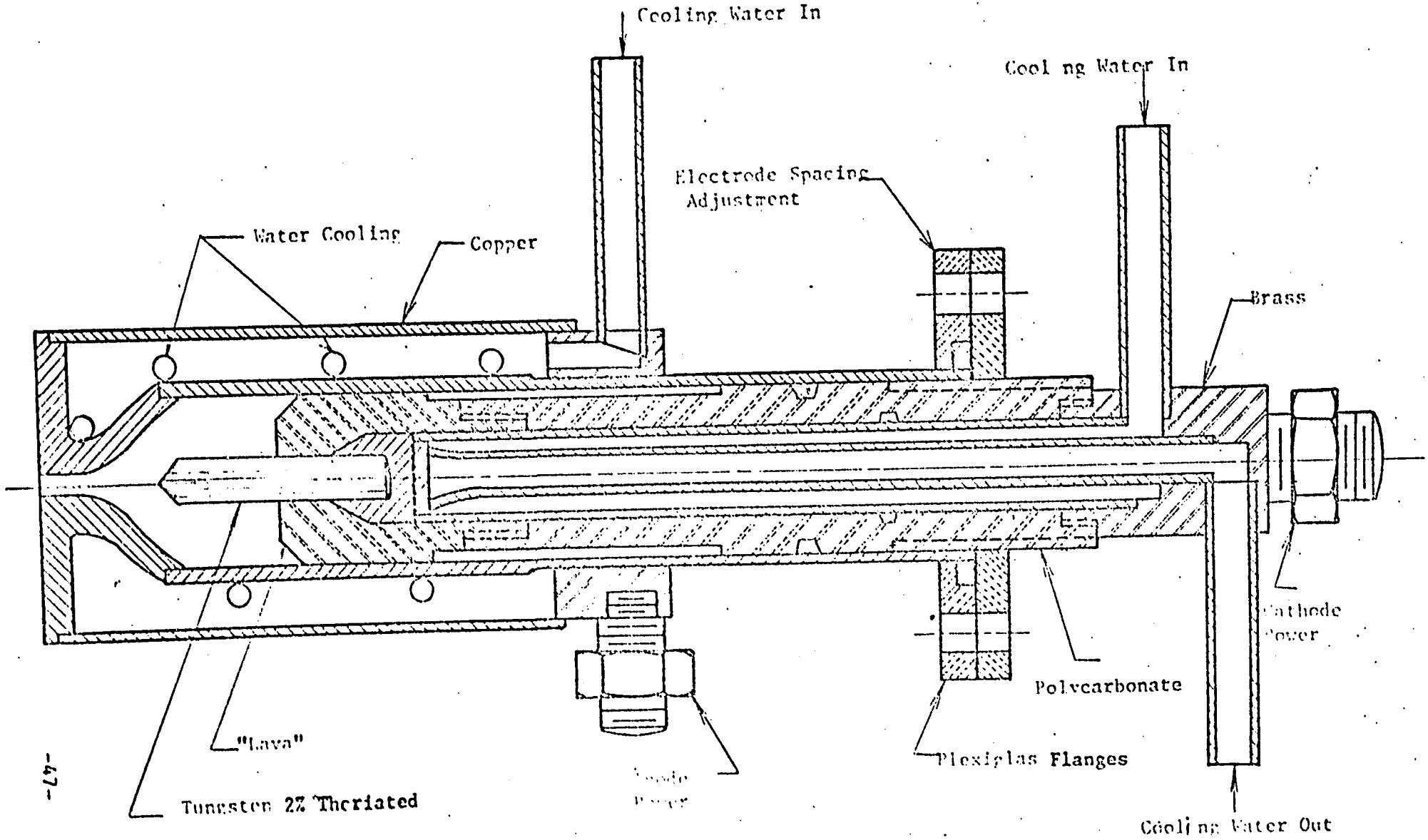

Figure 11: Design of Arc Jet. Scale 1:1

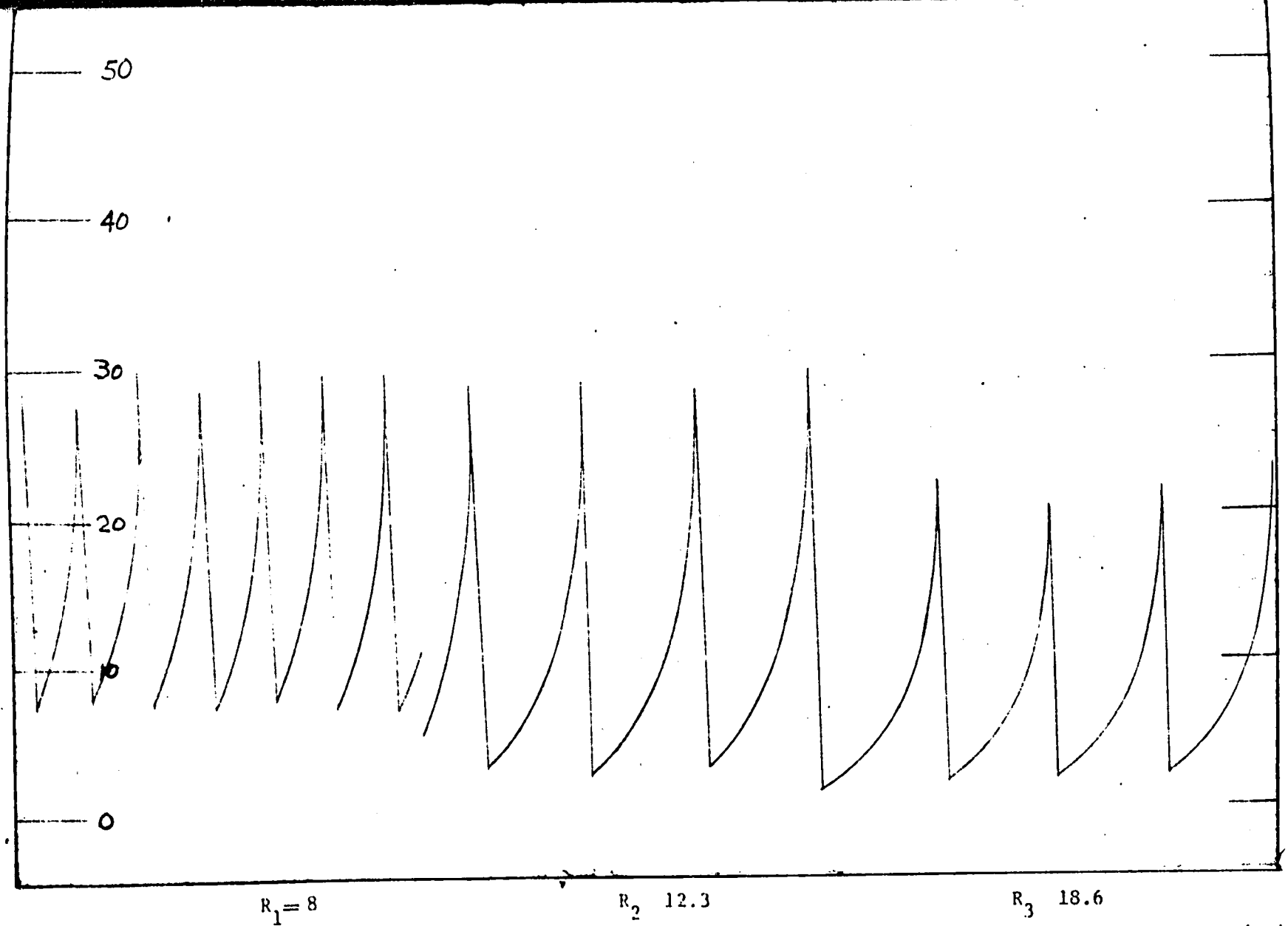

1/8 inch Jet Nozzle Diameter, 10 cuft/hr Flow Rate (Reproduction)
75 amp Arc Current, 0.75 inch from the Nozzle
T_1=993°k

Figure 12: (a) Viscorder Trace of Output from 0.025 inch Diameter Thermocouple Bead.

Diameter Thermocouple Bead.

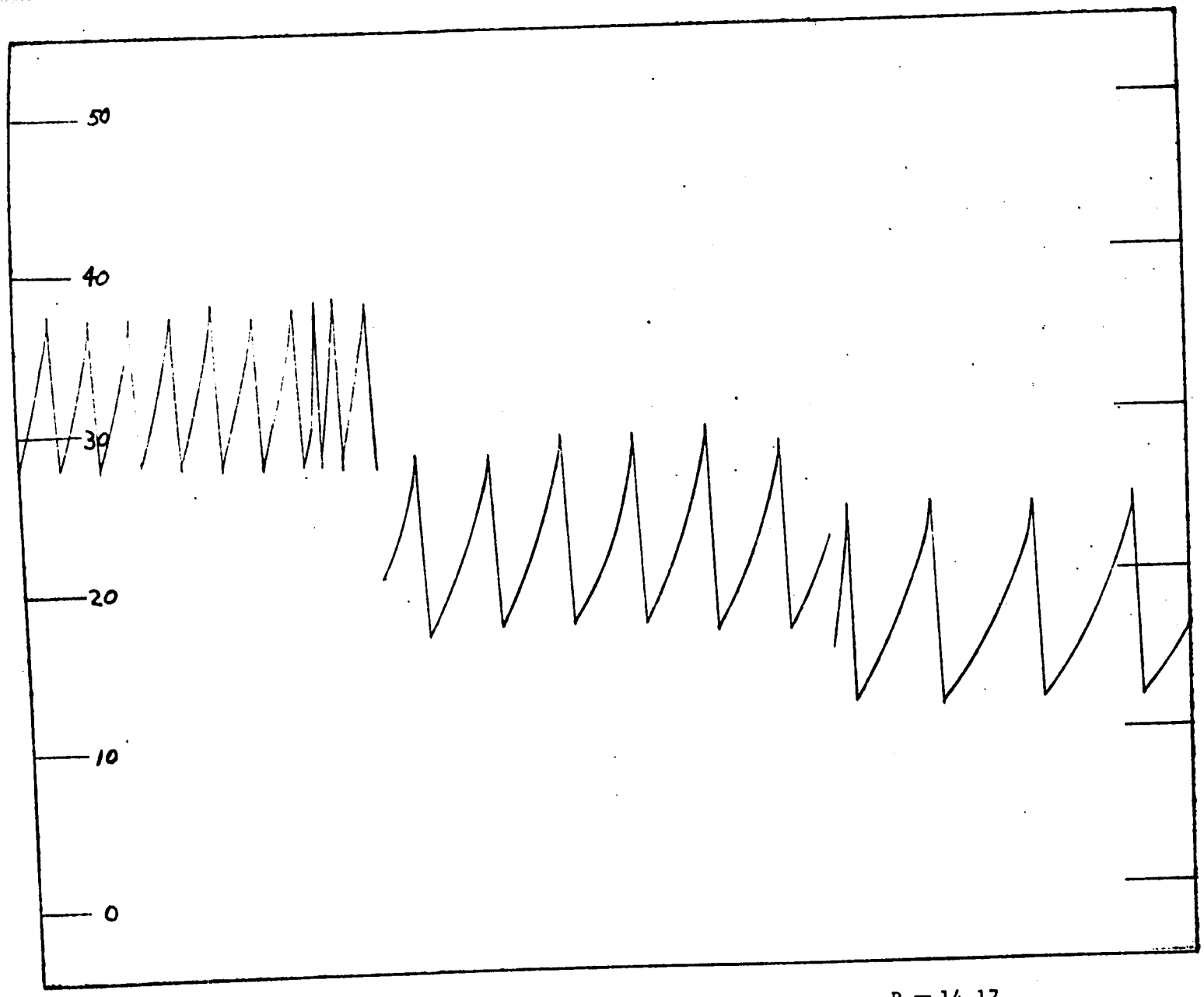

0.177 inch Jet Nozzle Diameter, 15 cuft/hr Flow Rate (*Reproduction*)
125 amp Arc Current, 0.625 inch from the Nozzle.
$T_1 = 1700°k$

Figure 12: (b) Viscorder Trace of Output from 0.063 inch Diameter Thermocouple Bead.

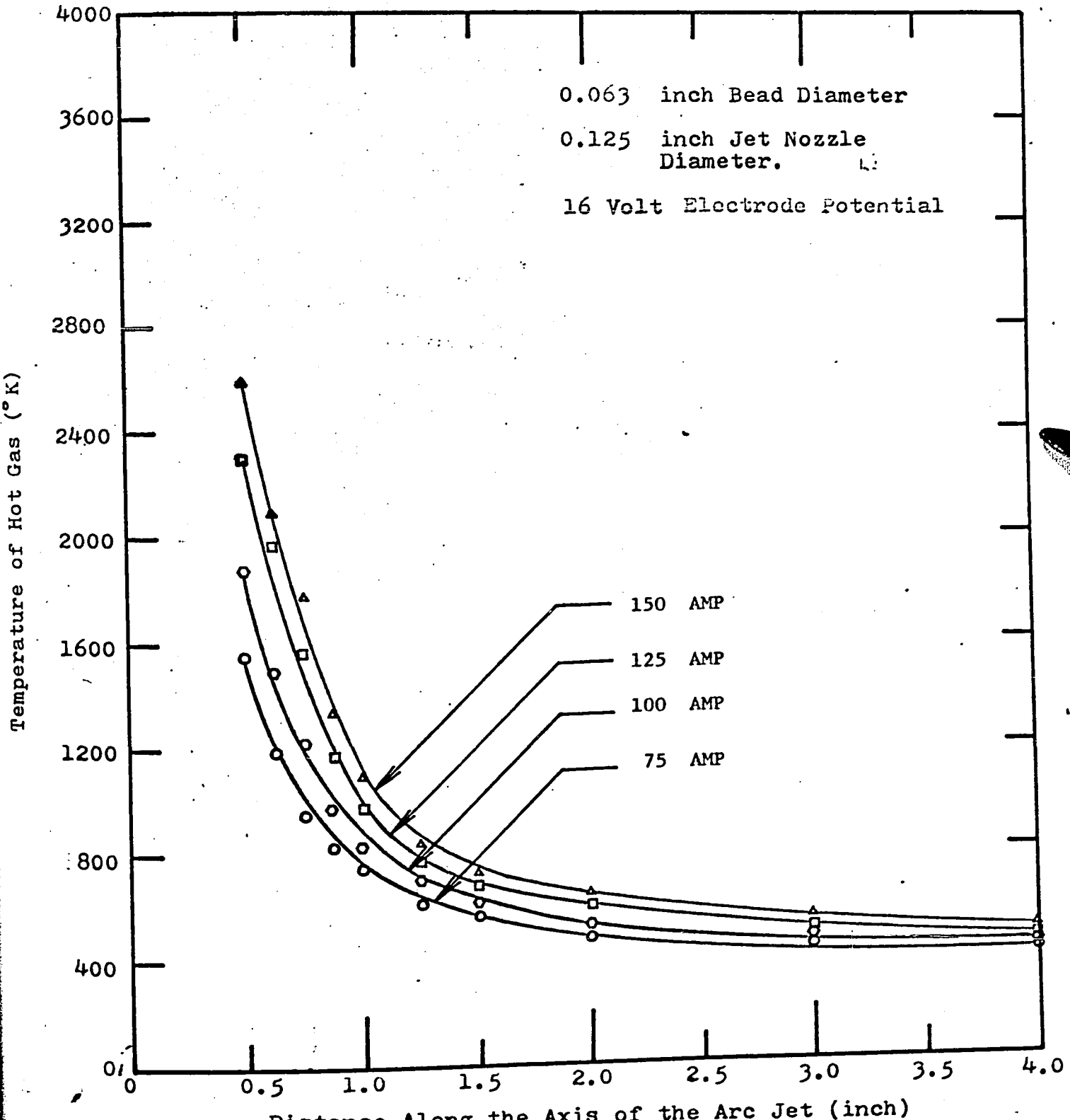

Figure 13: Axial Plasma Jet Temperature Profiles (o.125 inch Nozzle Diameter, 10 cuft/hr Flow Rate).

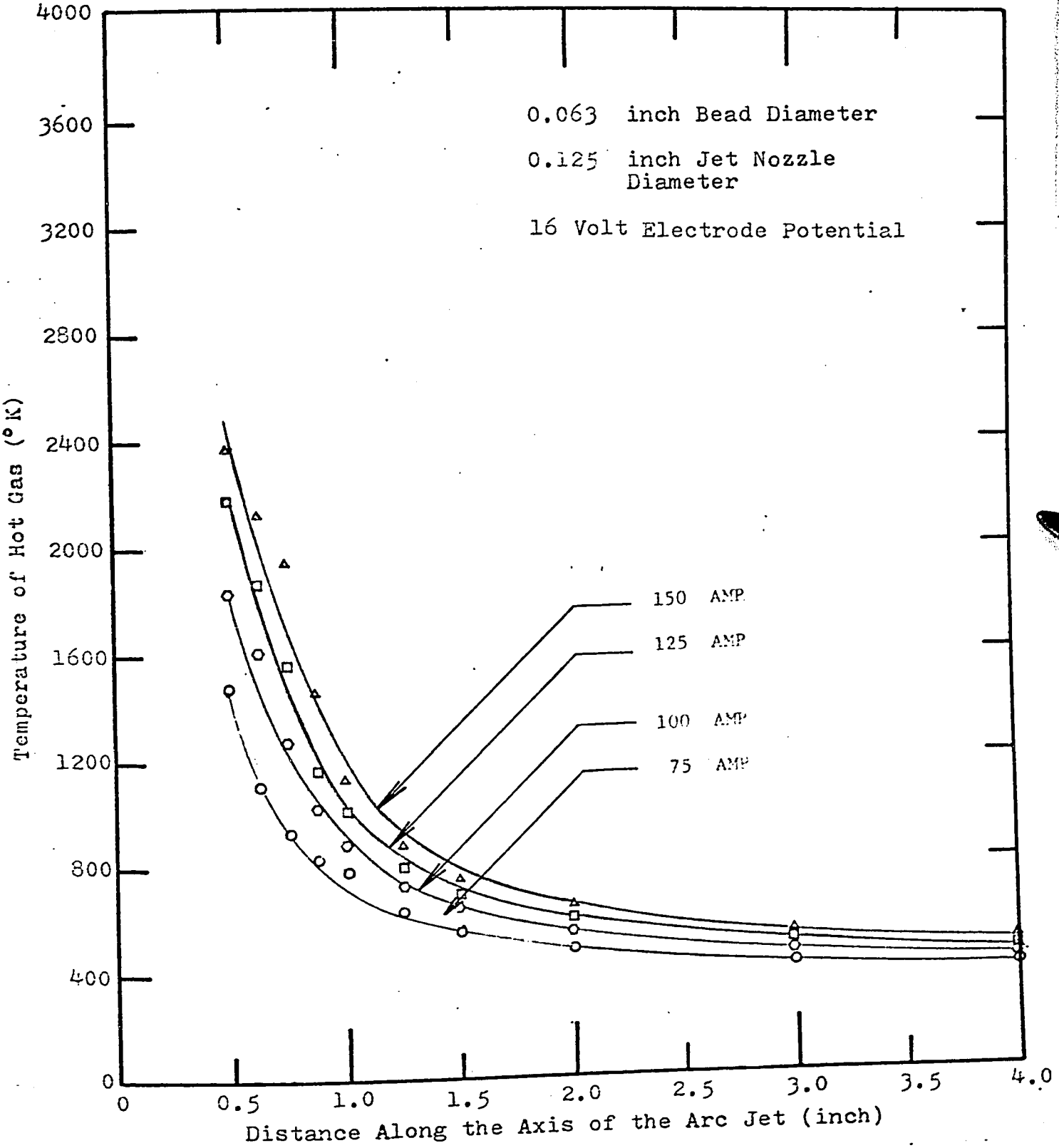

Figure 14: Axial Plasma Jet Temperature Profiles (0.125 inch Nozzle Diameter, 15 cuft/hr Flow Rate).

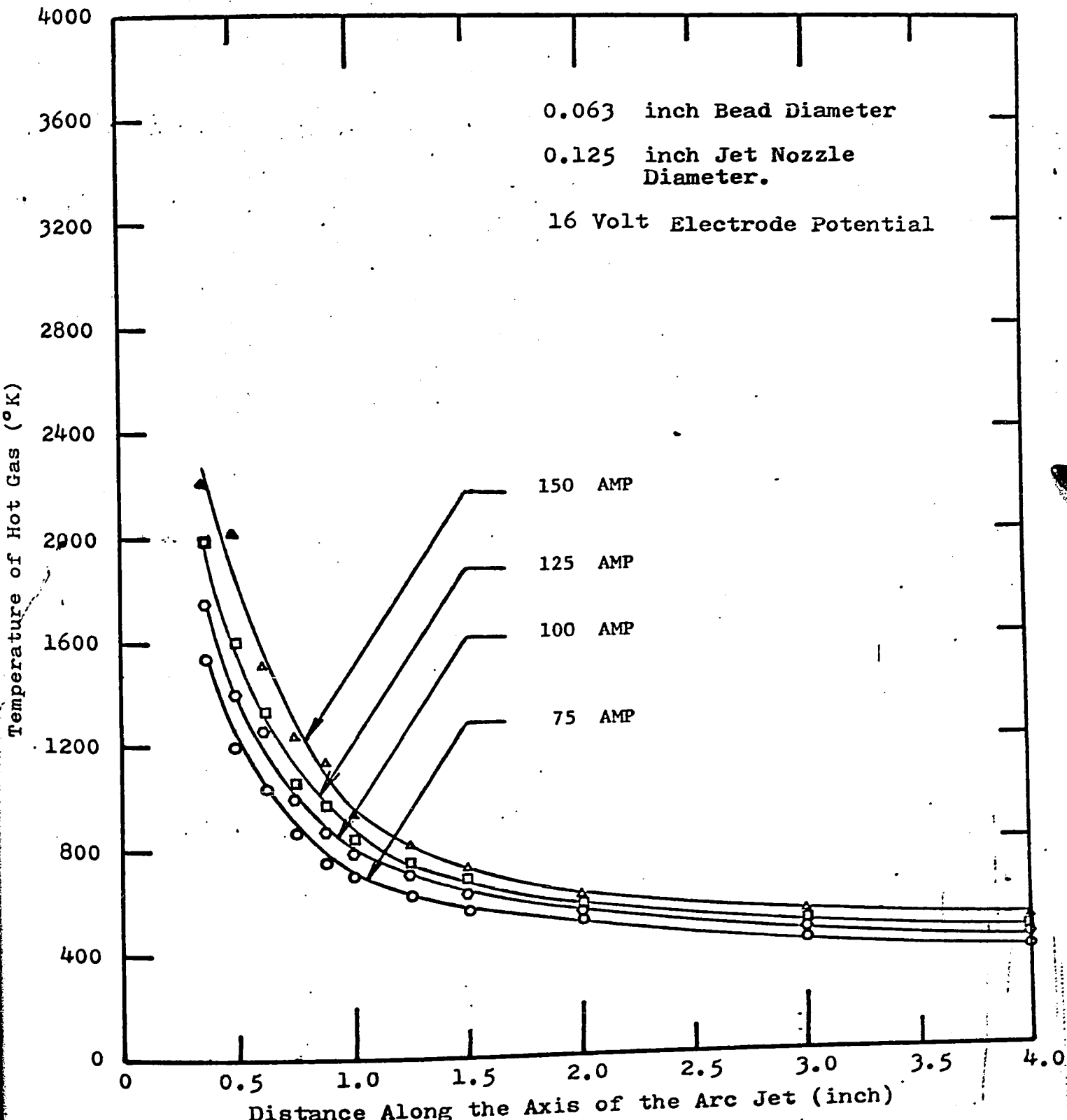

Figure 15: Axial Plasma Jet Temperature Profiles (0.125 inch Nozzle Diameter, 20 cuft/hr Flow Rate).

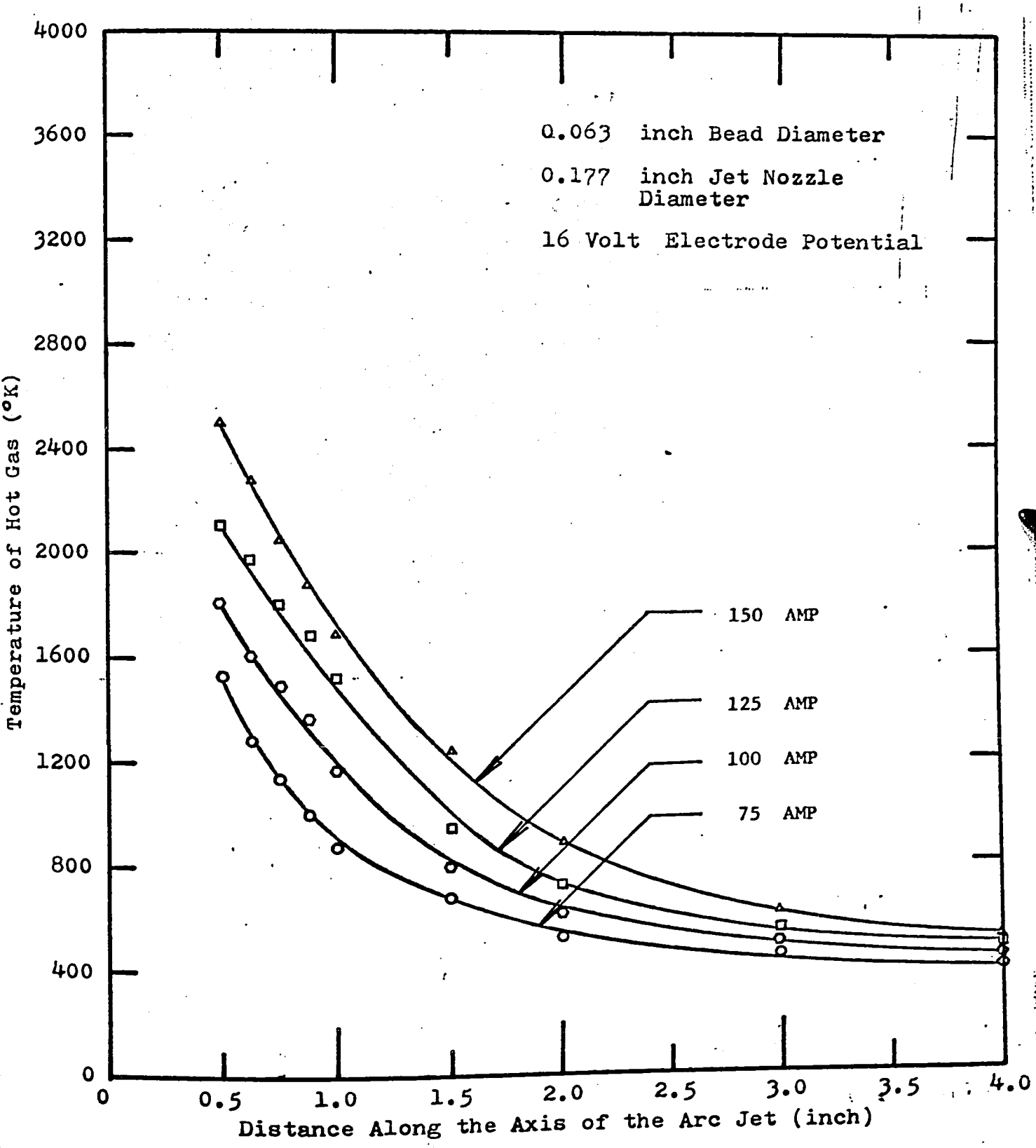

Figure 16: Axial Plasma Jet Temperature Profiles (0.177 inch Nozzle Diameter, 10 cuft/hr Flow Rate).

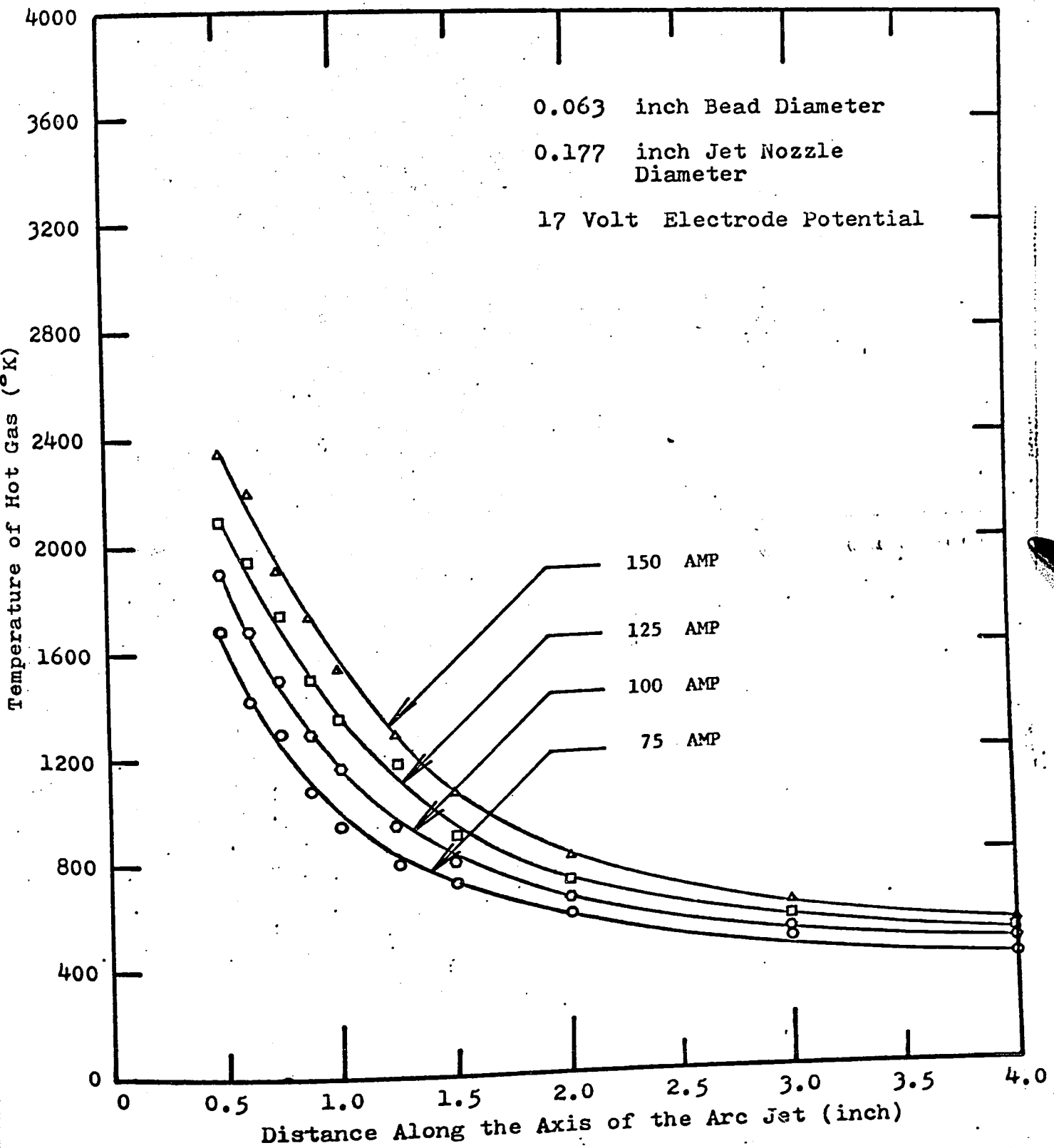

Figure 17: Axial Plasma Jet Temperature Profiles (0.177 inch Nozzle Diameter, 15 cuft/hr Flow Rate).

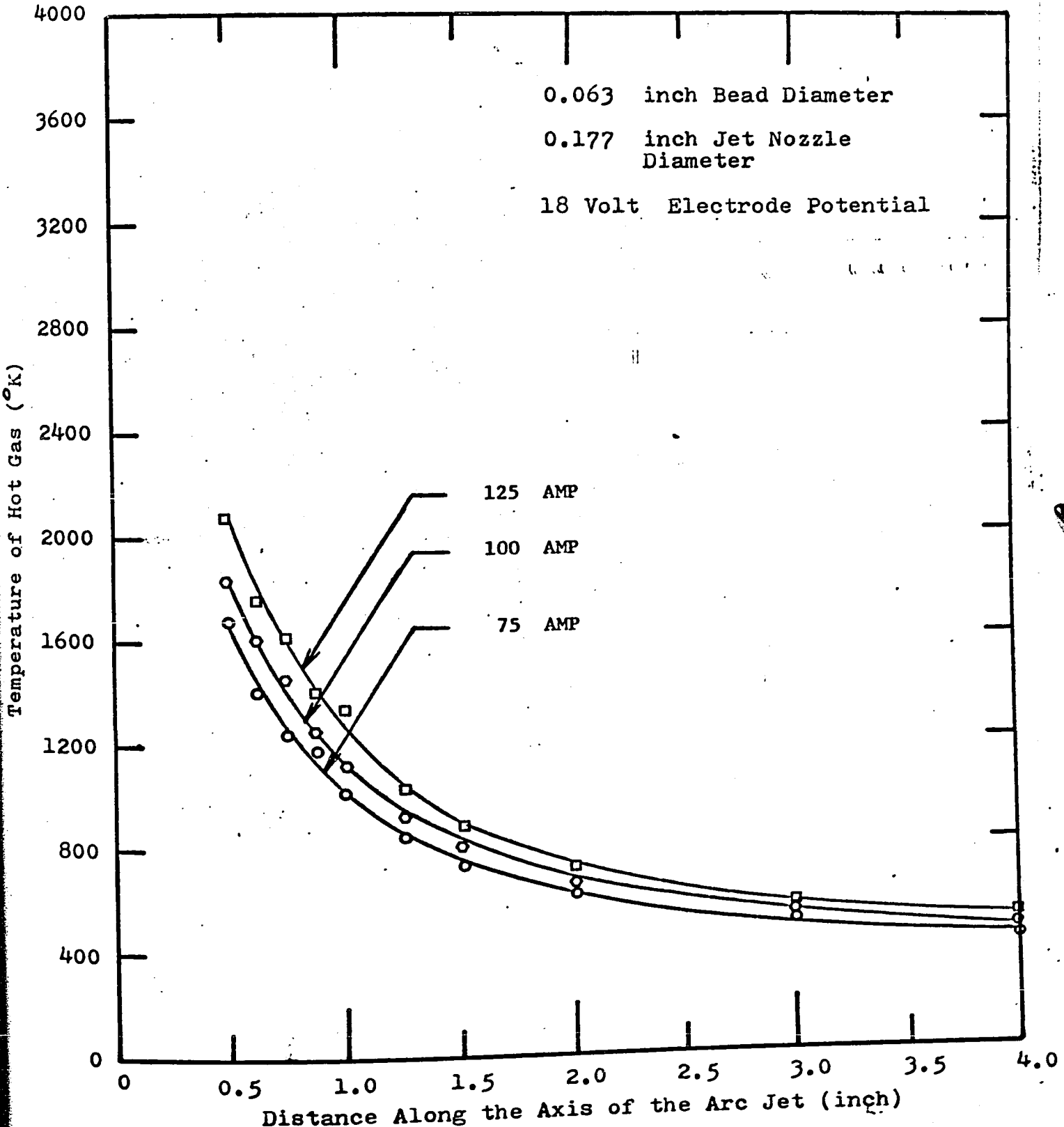

Figure 18: Axial Plasma Jet Temperature Profiles (0.177 inch Nozzle Diameter, 20 cuft/hr Flow Rate).

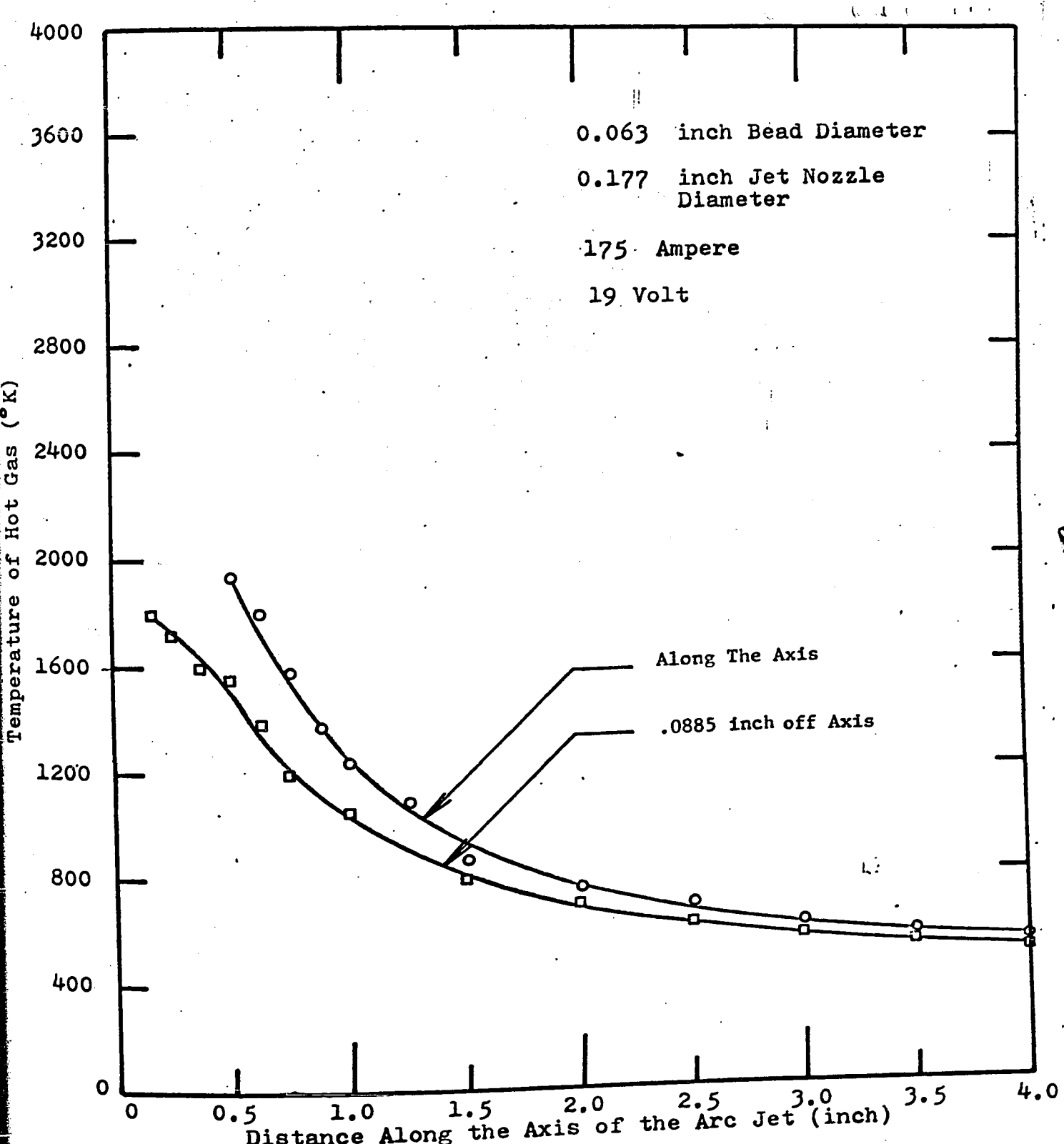

Figure 19 Axial and 0.0885 inch Off-Axial Plasma Jet Temperature Profiles (0.177 inch Nozzle Diameter, 25 cuft/hr Flow Rate, 175 ampere).

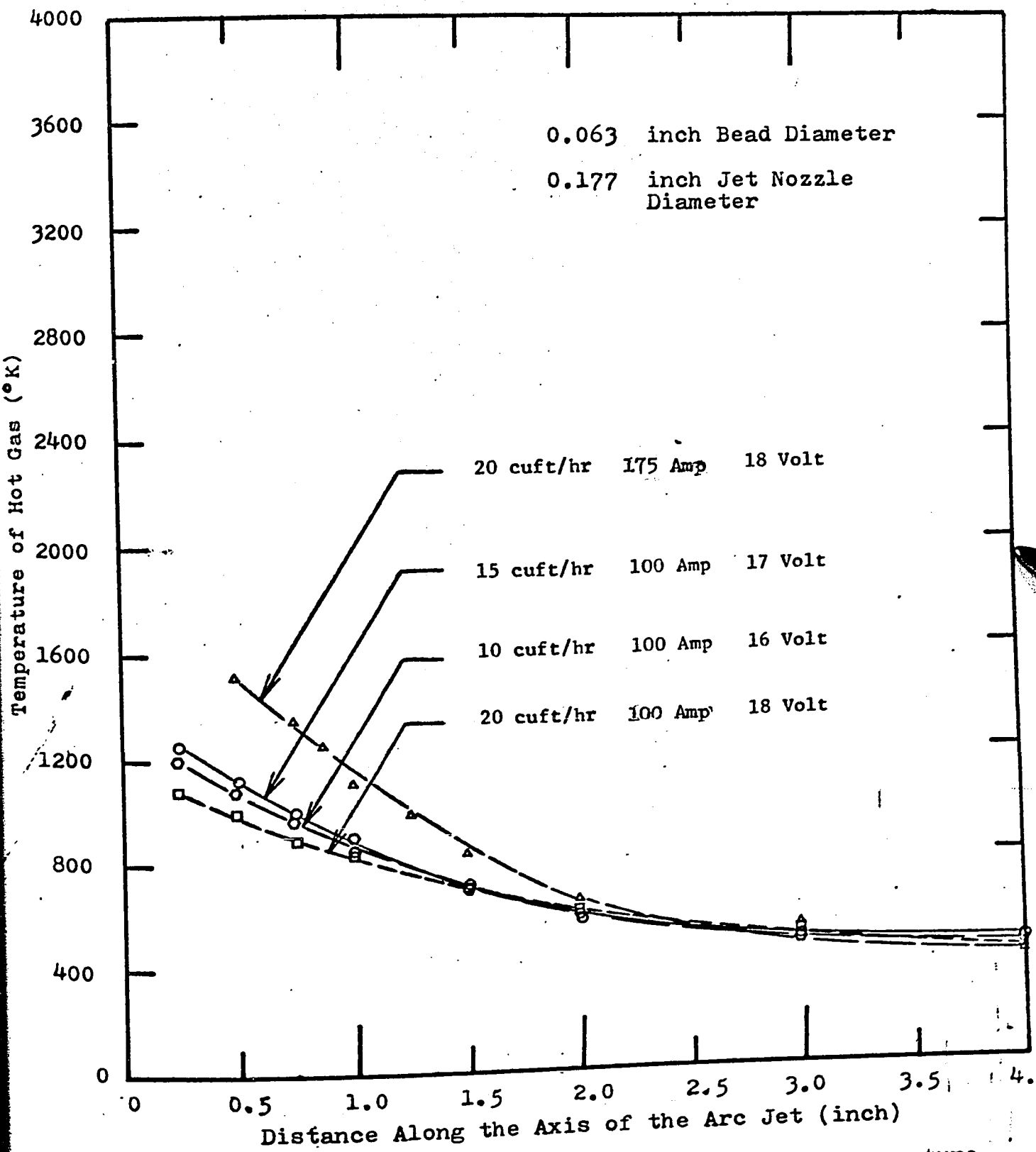

Figure 20: 0.0885 inch Off-Axial Plasma Jet Temperature Profiles.

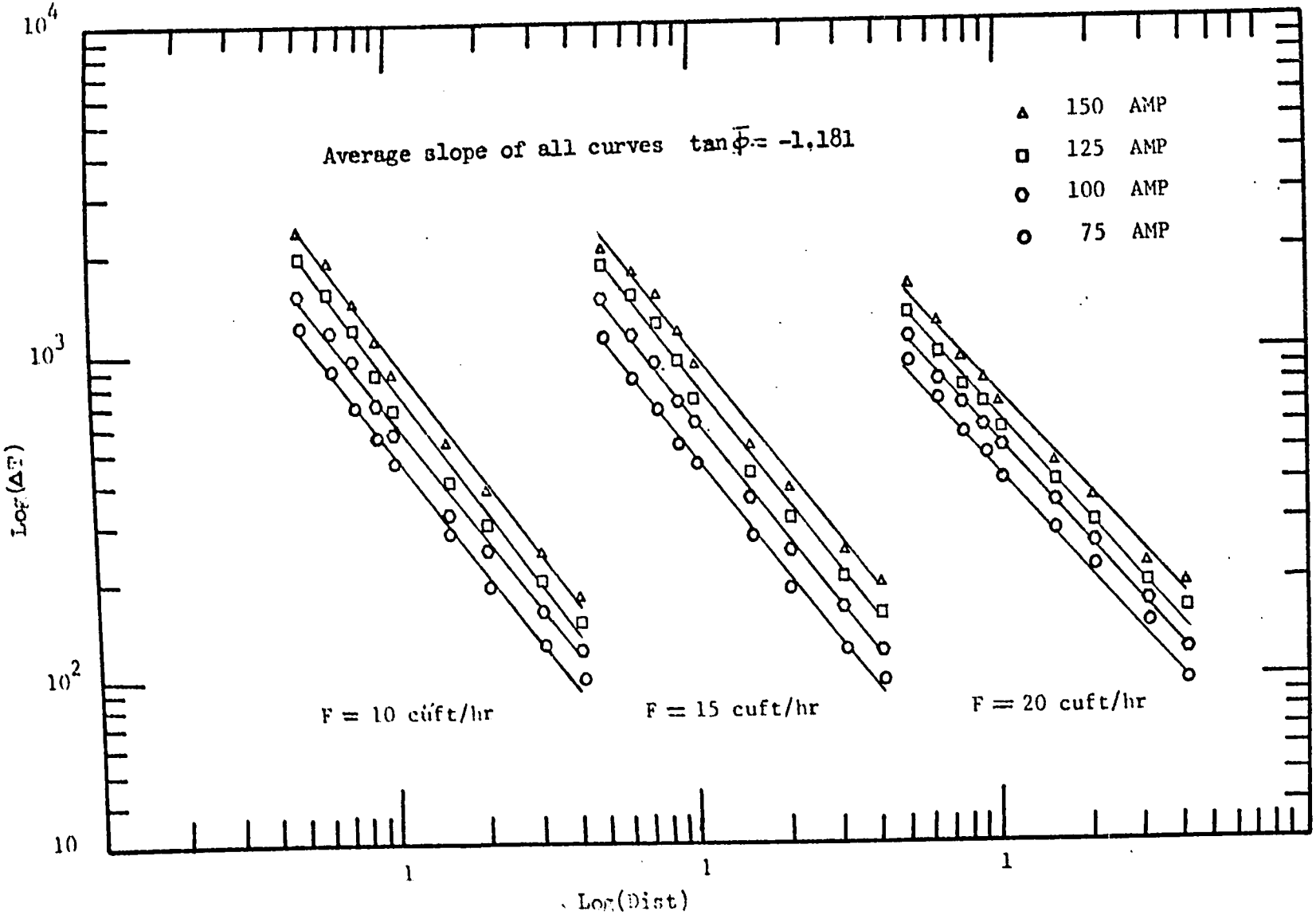

Figure 21: Log(Δ T) vs Log(Dist) Plot of the Data.

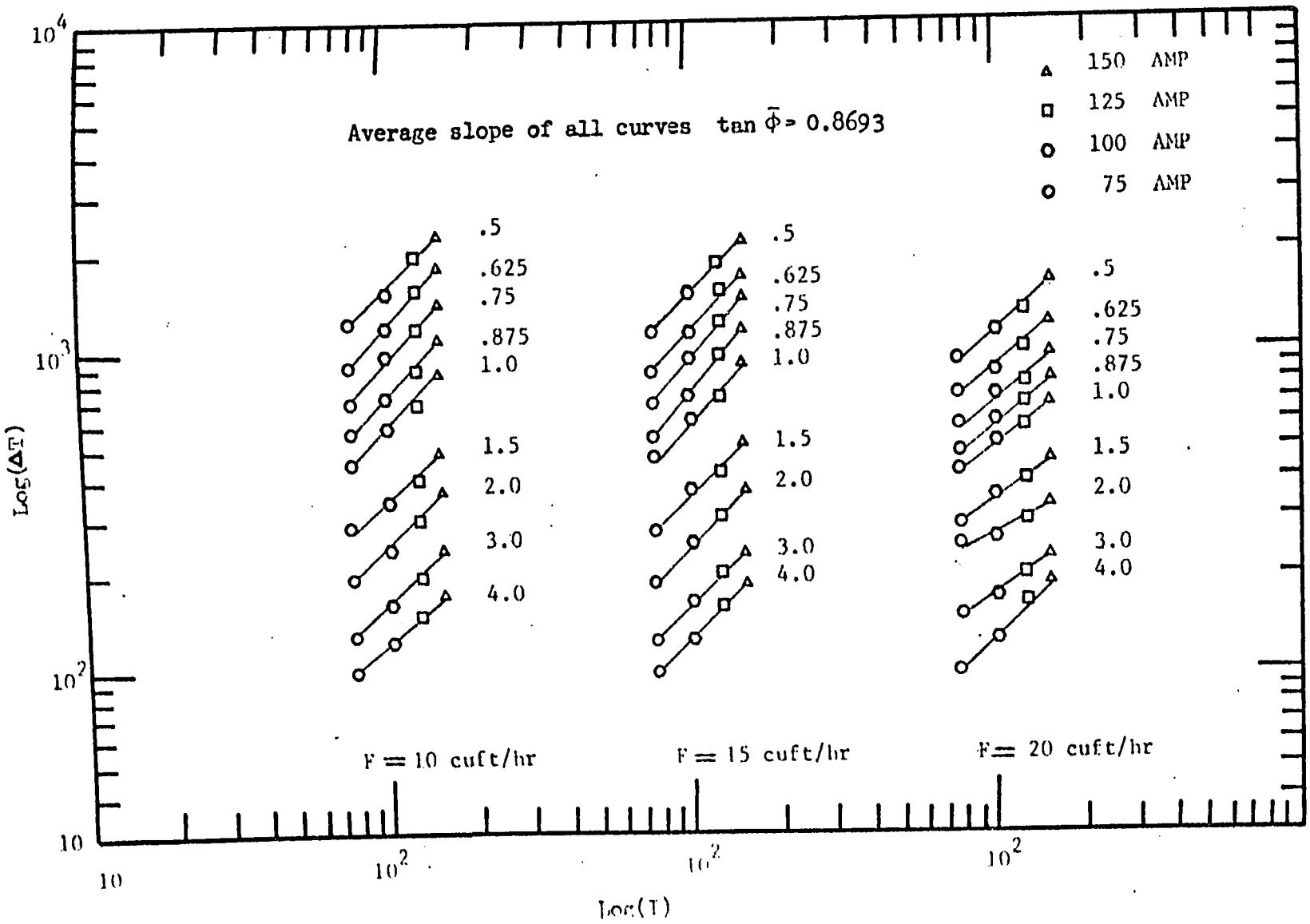

Figure 22: Log(Δ T) vs Log(I) Plot of the Data.

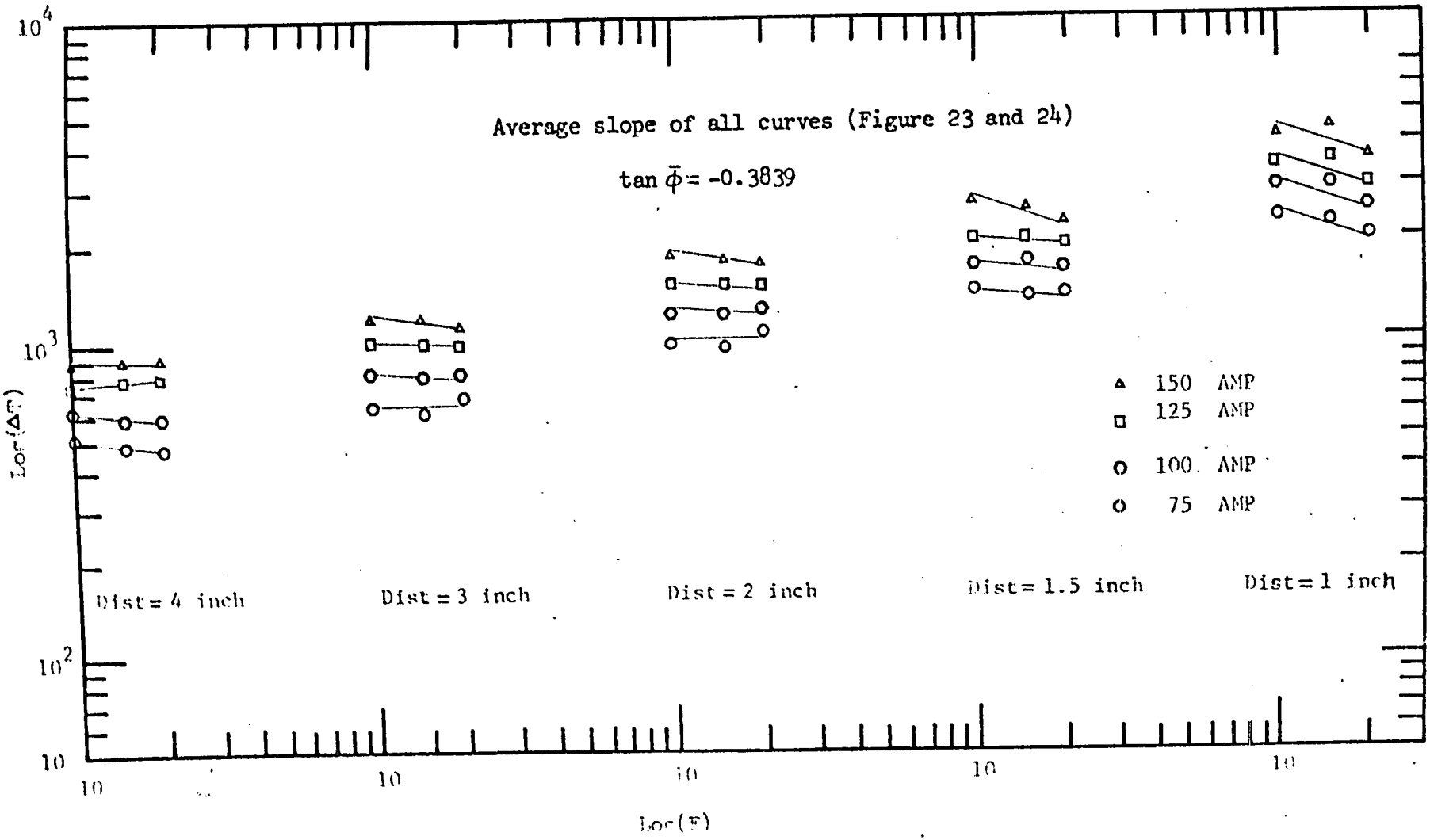

Figure 23: Log(ΔT) vs Log(F) Plot of the Data.

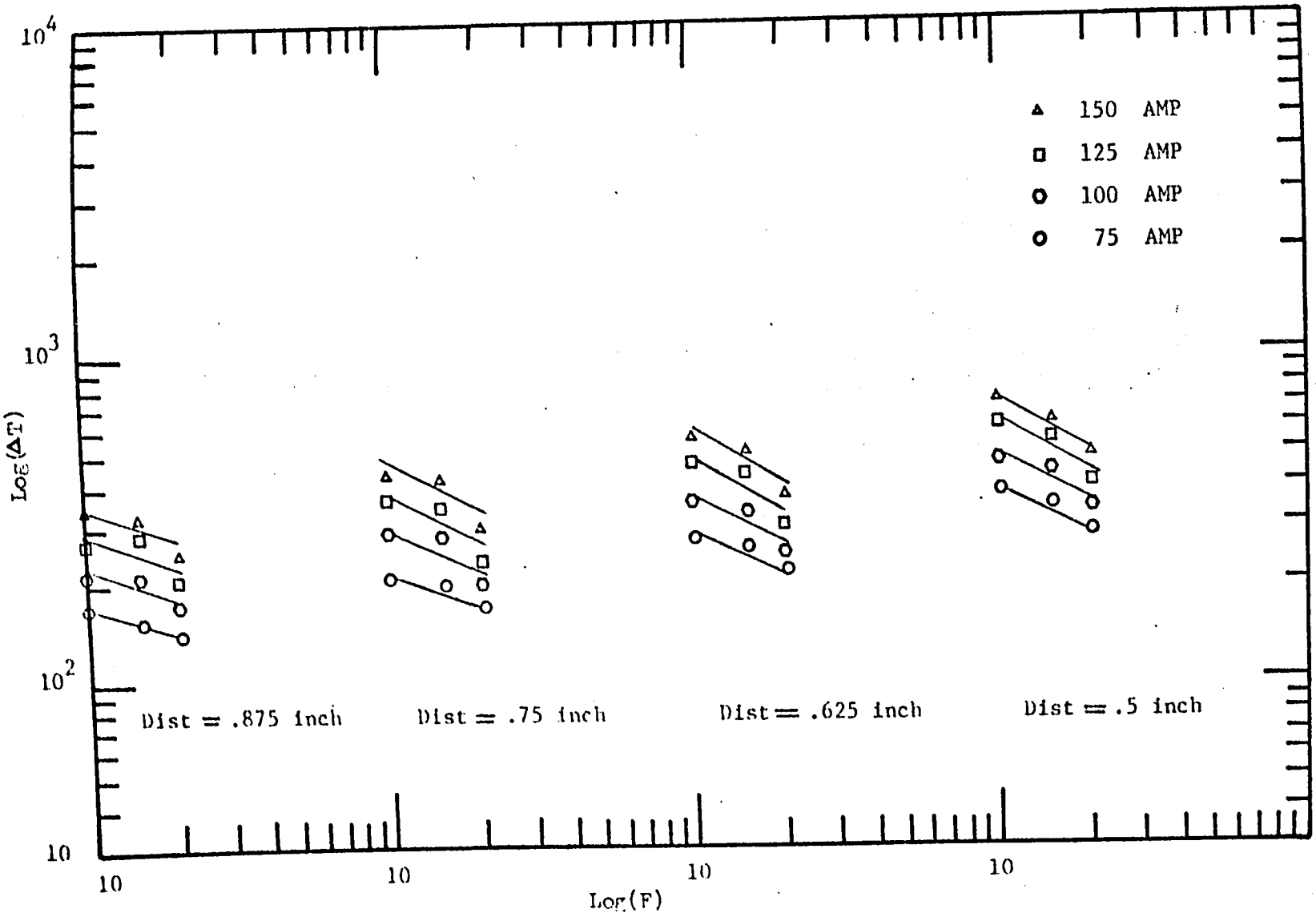

Figure 24: Log(ΔT) vs Log(F) Plot of the Data.

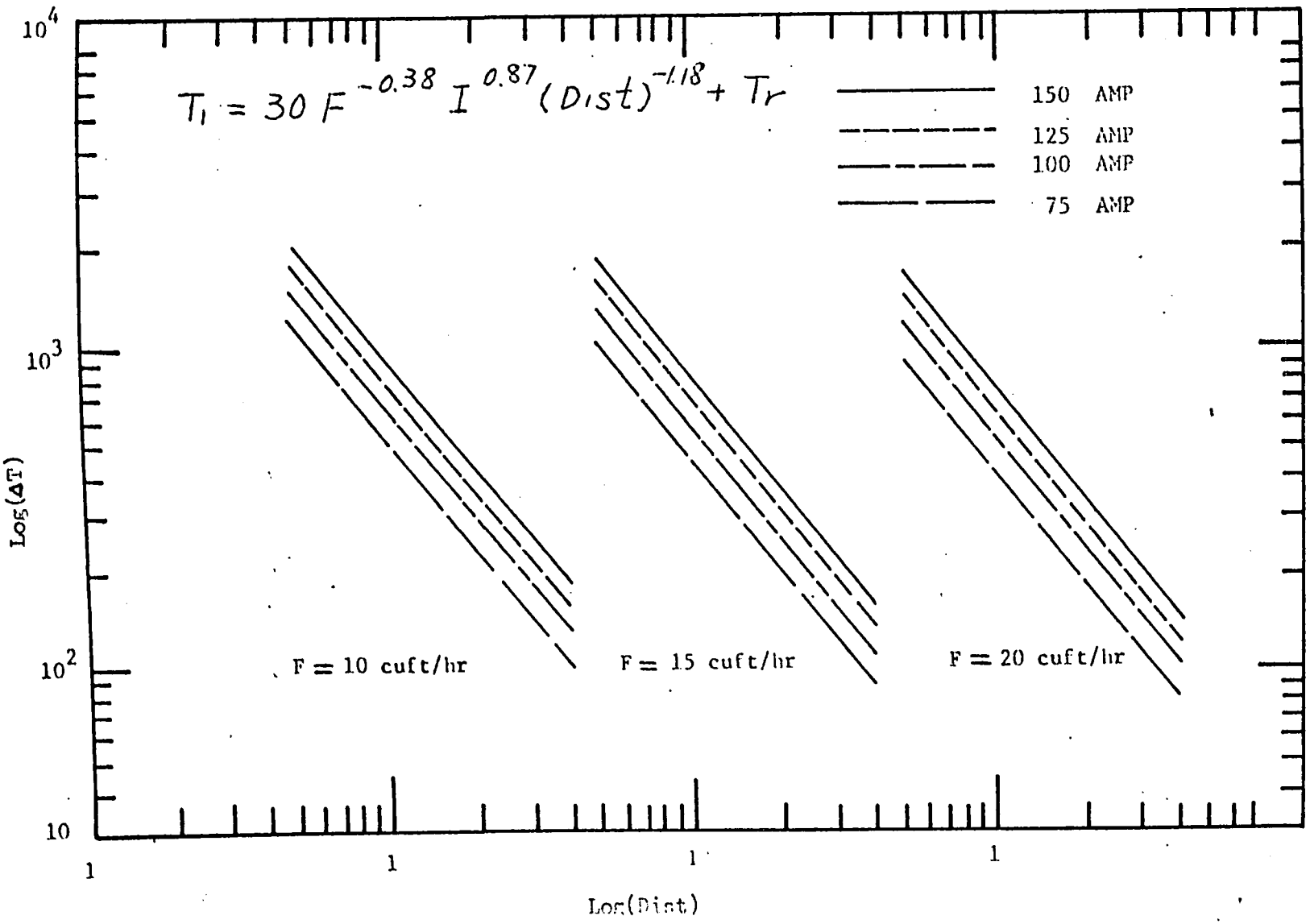

Figure 25: Log(Δ T) vs Log(Dist) Plot of Equation (44)

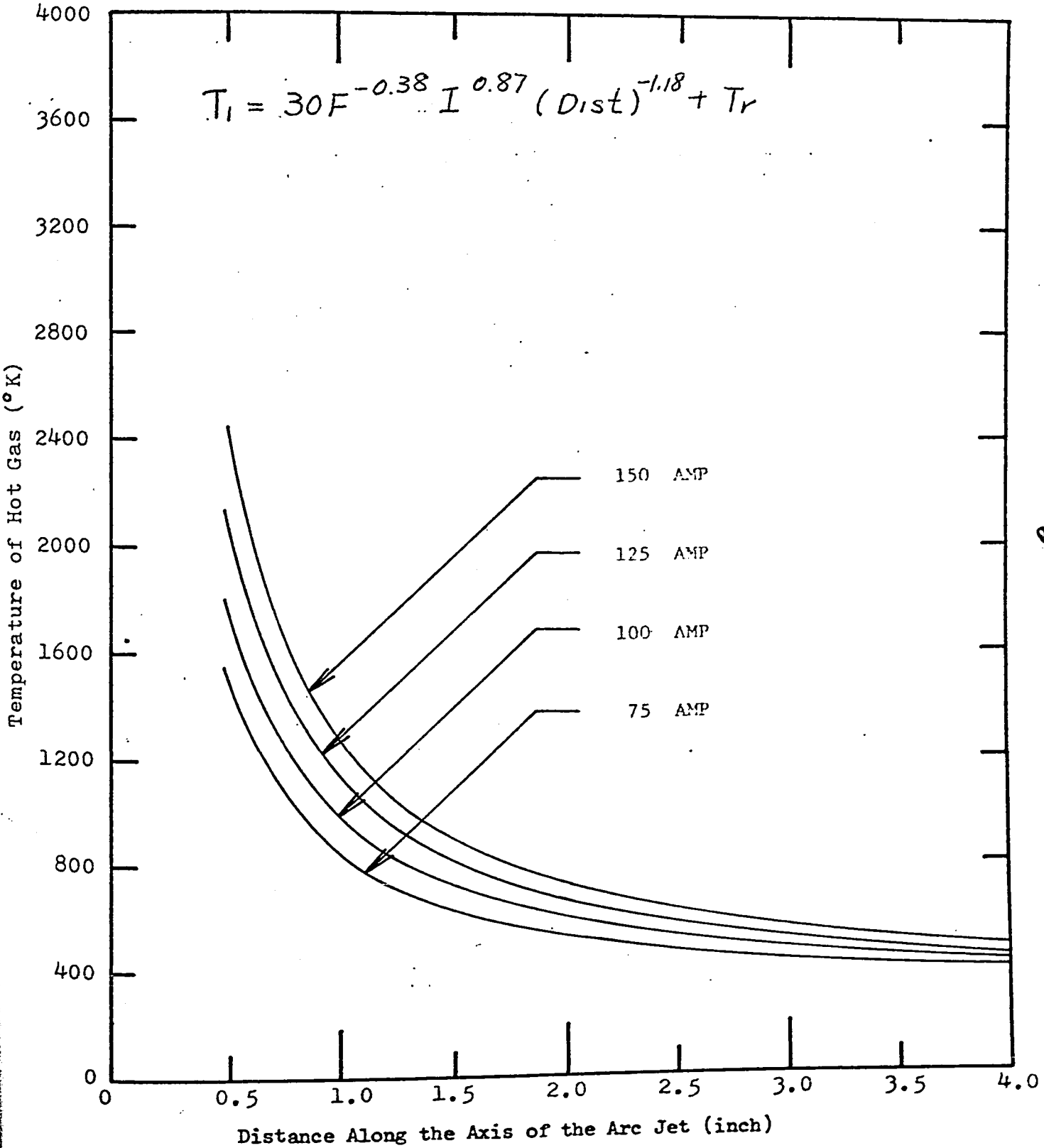

Figure 26: Axial Plasma Jet Temperature Profiles as Given by Empirical Equation (44).
(10 cuft/hr Flow Rate).

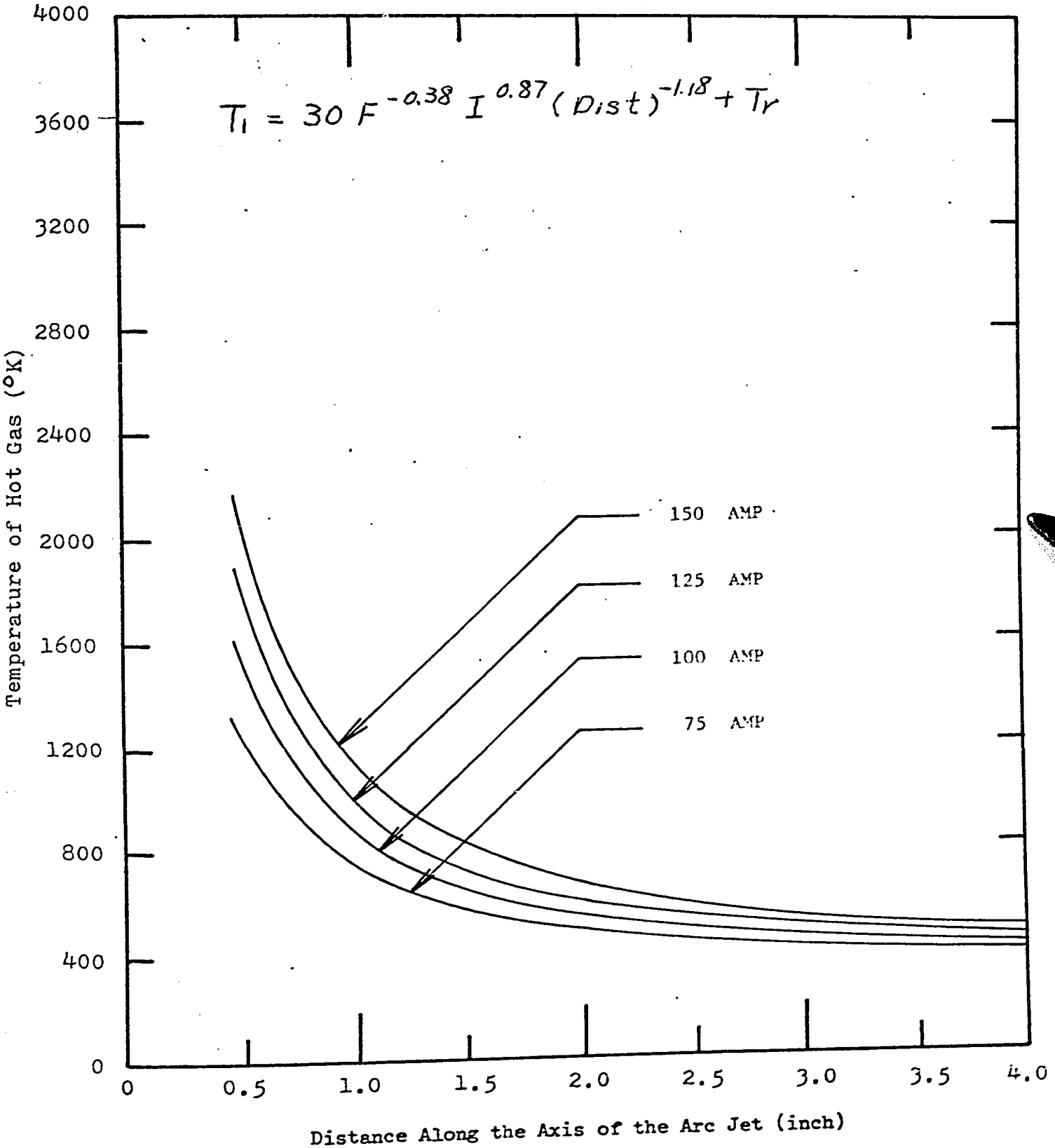

Figure 27: Axial Plasma Jet Temperature Profiles as Given by Empirical Equation (44) (15 cuft/hr Flow Rate).

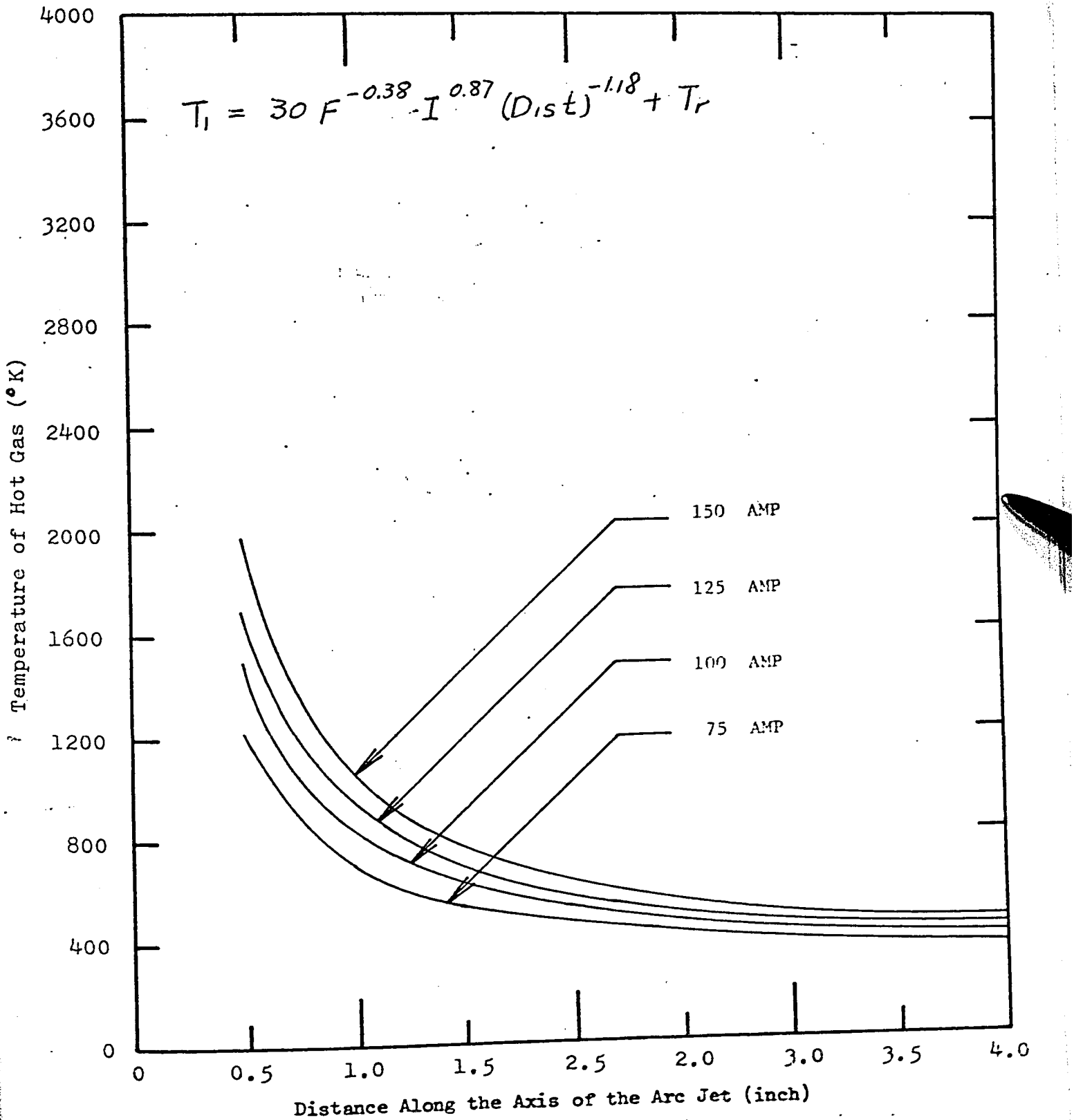

Figure 28: Axial Plasma Jet Temperature Profiles as Given by Empirical Equation(44)
(20 cuft/hr Flow Rate)

REFERENCES

1. Soundy, R. G. — "A Simple Electrostatic Probe for the Measurement of Ion Density in Atmospheric Pressure Flames and Its Application to a Study of Charge Exchange Reactions in Hydrocarbon Flame Gas". AGARD. Fundamental Studies of Plasma, Vol. 1, (Sept. 1965)

2. Grey, J. Jacobs, P. F. — "Calorimetric Probe for the Measurement of Extremely High Temperature". Review of Scientific Instruments, Vol. 33, No. 7, pp. 738-741, (July 1962)

3. Grey, J. Jacobs, P. F. — "Cooled Electrostatic Probe", AIAA J., Vol. 5, No. 1, pp. 84-90, (Jan. 1967)

4. Raezer, S. D. Olsen, H. L. — "The Intermittent Thermocouple: A New Technique for the Measurement of Extreme Temperature", Temperature and Its Measurement and Control in Science and Industry", Vol. 3, Part 2, (1962)

5. Henry, R. P. — "Ion-Slip Limitations on Currents in Hall Effect Plasma Accelerators", Ph.D. Thesis, Dept. of M. E., U. of T. (1968)

6. Bennett, W. L. Gayheart, E. L. Olsen, H. L. — "A Method of Temperature Measurement of Incipient Flame Kernels", Applied Phy. Laboratory, The John Hokin University Report C. M. 815, (Aug. 1954)

7. Schenck, H. Jr. — "Theories of Engineering Experimentation" McGraw-Hill Inc., (1968)

8. Loth, J. L. — "Thermal Radiation Energy Transfer From Very High Temperature Plasmas", Ph. D. Thesis, Dept. of Mechanical Engg, U. T. (1962)

9. Jacobs, P. F.
Grey, J.
"Measurements of Total Energy Radiated from an Argon Arc Jet", Technical Report No. 621, Aeronautical Engineering Lab., Princeton, (Aug. 1962)

10. Bradley, D.
Mathews, K. J.
"Measurement of High Gas Temperature with Fine Wire Thermocouples", Journal of Mech. E. Science, Vol. 10, No. 4, (1968)

11. Hinze, J. O.
Turbulence, McGraw-Hill, pp. 76, (1959)

12. Glawe, G. E.
Simmons, F. S.
Stickney, T. M.
"Radiation and Recovery Correction and Time Constants of Several Chromel-Alumel Thermocouple Probes in High Temperature High Velocity Gas Stream", NACA TN 3766, (Oct. 1956)

13. Cambell, A. B.
Plasma Physics and Magnetofluidmechanics, McGraw-Hill Book Company, (1963)

14. Holman, J. P.
Heat Transfer, McGraw-Hill Book Company, Inc., pp. 274, (1963)

15. Jahn, R. G.
Physics of Electric Propulsion, McGraw-Hill Book Company, (1968)